Available online at www.sciencedirect.com
SCIENCE DIRECT®
Journal of Colloid and Interface Science 273 (2004) 39–63
JOURNAL OF Colloid and Interface Science
www.elsevier.com/locate/jcis

Estimating the pore size distribution of activated carbons from adsorption data of different adsorbates by various methods

Piotr A. Gauden,[a,b] Artur P. Terzyk,[a,*] Gerhard Rychlicki,[a,b] Piotr Kowalczyk,[c] Magdalena S. Ćwiertnia,[a] and Jerzy K. Garbacz [b]

[a] *Physicochemistry of Carbon Materials Research Group, Department of Chemistry, N. Copernicus University, Gagarina 7, 87-100 Toruń, Poland*
[b] *Department of Environment Protection, Academy of Humanities and Economics, Okrzei 9, 87-800 Włocławek, Poland*
[c] *Department of Chemistry, Faculty of Science, Chiba University, 1-3 Yayoi, Inage, Chiba 263, Japan*

Received 3 July 2003; accepted 20 August 2003

Abstract

Experimental adsorption isotherms of four adsorbates (N_2, Ar, C_6H_6, and CCl_4) as well as adsorption enthalpy (C_6H_6 and CCl_4) measured on two strictly microporous carbons are used to evaluate the porosity of adsorbents (i.e., pore size distributions (PSDs) and average pore diameter (L_{av})). The influence of the diameter of adsorbates (d_A) as well as of the temperature (T) is analyzed in order to explain the differences or similarities between the above-mentioned quantities for all systems. Proposed previously, the general relationships between the parameters of the Dubinin–Astakhov (DA) isotherm equation (the characteristic energy of adsorption (E_0) and the exponent of this equation (n)) and the average slit-width of carbon micropores are investigated. Moreover, the thermodynamic verification of the Horvath–Kawazoe (HK) theory and the ND model is presented based on data of the adsorption and enthalpy of adsorption of benzene and carbon tetrachloride on two carbons. Finally, the pore diameters calculated from calorimetry data using the Everett and Powl method and those calculated applying the recently developed equations are compared. In our opinion the change of apparent PSD should be monitored by performing a series of isotherm measurements from high (equal and higher than room temperature) to low temperatures (ca. 77.5 K) as was presented in the current study. Moreover, the analysis of the experimental data leads to the conclusion that the entropy of C_6H_6 and CCl_4 can approach to the values characteristic of quasi-solid (a partially ordered structure). Therefore, this behavior of the adsorbate should be taken into consideration in the theoretical assumptions of model and its thermodynamic verification.

Keywords: Adsorption; Active carbon; Microporosity; Pore width; The Horvath–Kawazoe theory, DFT; The Nguyen–Do model; Potential theory; Calorimetry; Thermodynamics of adsorption; Molecular sieve effect

1. Introduction

Usually information on the micropore system of the investigated adsorbents can be obtained from Dubinin's theory of the volume filling of micropores (TVFM), applying, for example, the Dubinin–Astakhov (DA) [1] equation,

$$\Theta = \exp\left[-\left(\frac{A_{pot}}{\beta E_0}\right)^n\right], \tag{1}$$

where $A_{pot} = RT\ln(p_s/p)$; p and p_s are the equilibrium and the saturation pressure, respectively; R and T are the gas constant and the temperature, respectively; Θ is the degree of micropore filling; β is the affinity coefficient (the specific parameter of the system under investigation depending on the adsorptive only, and it has been assumed that $\beta(C_6H_6) = 1$); E_0, the characteristic energy, and n, the exponent of the above-mentioned equation, are the best-fit parameters. It should be pointed out that the DA equation possesses limitations [2–5]; however, it still occupies the leading position in the adsorption field [4–8]. For carbonaceous adsorbents the values of the exponent n lie usually in the range 1–3, depending strongly upon the type of adsorbent [6,9–11]. Values of n approaching three and higher are the most frequently found in the literature for adsorbents with narrow micropores of small size range, while values of n approaching one are found for adsorbents with a wide range of pore sizes [6,9–11].

* Corresponding author.
E-mail address: aterzyk@chem.uni.torun.pl (A.P. Terzyk).

0021-9797/$ – see front matter
doi:10.1016/j.jcis.2003.08.033

The simplest method of microporosity characterization is the application of the relation between the average micropore diameter of the slit-shaped micropores (L_{av}) and E_0. Plenty of such relations have been proposed on the basis of both semi-theoretical and experimental research [12–26]. On the basis of the set of independent data obtained from the adsorption an immersion techniques and from small-angle scattering of X-rays (SAXS), Dubinin proposed at the beginning of the 1980s a simple inversely proportional relationship between E_0 and L_{av} [12]. Later, this relation was slightly modified by Dubinin and Stoeckli [15] and intensively investigated by Bhatia and Shethna [13] and Kadlec [14],

$$L_{av} = \frac{\kappa}{E_0}, \tag{2}$$

where κ is the characteristic constant for a defined adsorbate/adsorbent pair in the micropore region [12,13]. The value of this characteristic constant for benzene vapor on activated carbon is about 12 kJ nm mole^{-1} [12,13]. It has been also assumed that this parameter is in a small degree dependent on the characteristic energy of adsorption [14],

$$L_{av} = \frac{13.028 - 1.53 \times 10^{-5} E_0^{3.5}}{E_0}. \tag{3}$$

Next, others relations were developed since this turning point. The intensive investigations were done by McEnaney [16,20],

$$L_{av} = 6.6 - 1.79 \ln(E_0), \tag{4}$$

$$L_{av} = 4.691 \exp[-0.0666 E_0], \tag{5}$$

Stoeckli and co-workers [17–19,21,22,24],

$$L_{av} = \frac{16.5}{E_0}, \tag{6}$$

$$L_{av} = \frac{18}{E_0}, \tag{7}$$

$$L_{av} = \frac{10.8}{E_0 - 11.4}, \tag{8}$$

$$L_{av} = \left(\frac{30}{E_0}\right) + \left(\frac{5705}{E_0^3}\right) + 0.028 E_0 - 1.49, \tag{9}$$

Choma and Jaroniec [23],

$$L_{av} = \left(\frac{10.416}{E_0}\right) + \left(\frac{13.404}{E_0^3}\right) + 0.008212 E_0 + 0.5114, \tag{10}$$

and Ohkubo et al. [26],

$$L_{av} = \frac{2 \times 10^3 V_{mi,\alpha}}{(S_{c,\alpha} - S_{me,\alpha})}, \tag{11}$$

where the parameters are calculated from the high-resolution α_s-plots method ($V_{mi,\alpha}$—the volume of micropores, $S_{c,\alpha}$—the total specific surface area, and $S_{me,\alpha}$—the specific surface area of mesopores).

In Fig. 1 the plots of the most widespread equations correlating E_0 and the micropore width (symbols) are shown in

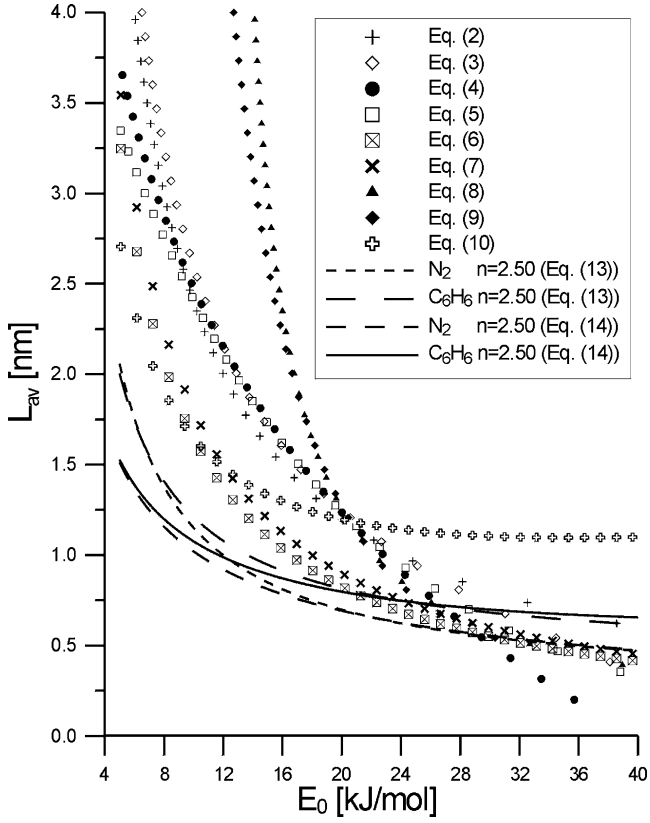

Fig. 1. The comparison of the predicted average pore diameters (using different empirical relations (Eqs. (2)–(10))-points) with calculated from theoretical relations proposed previously (Eqs. (13) and (14); C_6H_6 and N_2; lines).

the typical range (found in the literature) of the characteristic energy observed for carbonaceous adsorbents. All relationships $L_{av} = f(E_0)$ generate the decreasing hyperbolic-like function for the range of E_0 values shown in this figure. It can be concluded that the values of L_{av} evaluated based on the various relationships are sometimes significantly different one from the other. Moreover, this type of relation was usually derived from the experimental investigation. The sieve effect was studied based on the molecular adsorption probe data (adsorption from gaseous phase (helium, benzene, and others) and from liquid phase (methyl blue, caffeine, and others)) on microporous adsorbents with different pore structures. The latter was additionally characterized using for example HREM (high resolution electron microscopy), SAXS and other techniques. Fig. 1 clearly shows that there are differences between the results generated from relationships proposed by different authors however, there were no the attempts to elaborate the reasons causing them. The authors of the current study do not question the validity of the relations proposed by others. However, we want to underline that the main disadvantage of so far proposed equations is a wrong and misleading application of them. Namely, usually the values of the average pore diameter of investigated adsorbents are calculated for the experimental systems being different as those considered during the

derivation of the relations. Moreover, the same equations can be used for the various adsorbates differing first of all, in the diameter and with other physicochemical constants. On the other hand, it should be also pointed out that carbons possess very complicated porous structure and the assumption of simple slit-like geometry of pores is simplification. It is well known that there no exists the model of the structure of microporous carbon that can successfully explain all measured experimentally physical and chemical features of this material and the new models are still proposed [27]. The most important problem connected with the development of the relations between E_0 and L_{av} is, in our opinion, the type of the microporous structure of the studied carbons. Different authors used different carbons. Probably some of the carbons possessed fine micropores (where the primary micropore filling process occurs), others micropores where both primary and secondary micropore filling occurred. Therefore, the relationships between the characteristic adsorption energy and the pore diameter cannot be regarded as general, and the reasons mentioned above cause, in our opinion, the differences between the plots of the curves in Fig. 1.

On the other hand, as was shown previously [6,7,9–11, 28–37], it is necessary to take into account (in the relations $L_{av} = f(E_0)$) the parameter n of the DA equation (which has not been considered before in this class of equations). The significance of this parameter is the important problem of the theory of volume filling of micropores (TVFM). Chen and Yang showed that n is really a structural parameter of carbon [25,38]. Dobruskin [39], considering the physical meaning of the parameters of DA equation, noticed that n does not depend on the pore dimensions and it is determined only by the standard deviation of micropore sizes, hence, it characterizes the surface heterogeneity. Similar conclusion was also provided by Jagiełło and Schwarz [36], Condon [40,41] as well as other authors. Summing up, this parameter should be connected with the average size of micropores and the micropore size distributions (MSDs).

Therefore, in order to find the relationships $L_{av} = f(E_0, n)$, a procedure for linking the DA equation (Eq. (1)) (i.e., values of adsorption and/or relative pressure) and the effective pore diameter was proposed [7,28–34]. Horvath and Kawazoe [42,43] based on thermodynamic analysis, applying the potential derived by Everett and Powl [44], derived the equation [31–34,42–44]

$$\ln(p/p_s) = \frac{A_{HK}}{L-d}\left[\frac{B_{HK}}{(L-d/2)^3} - \frac{C_{HK}}{(L-d/2)^9} - D_{HK}\right], \tag{12}$$

where d is the sum of the diameter of an adsorbent (d_a) atom and an adsorbate molecule (d_A) (the remaining parameters of the above equation are defined in Appendix A and Table 1). Finally, the following two equations were obtained [7,29–34],

Table 1
The parameters characterizing adsorbates analyzed in the current paper (Ar, N_2, CCl_4, and C_6H_6) (the other values are given in [29,31,32])

Parameter	Adsorbate			
	Ar	N_2	CCl_4	C_6H_6
Diameter, d_A	0.336	0.300	0.465	0.459
Liquid density, ρ (g/cm^3)	1.465	0.808	1.565	0.861
Temperature, T (K)	77.50	77.50	308.00	313.15
Affinity coefficient, β	0.31	0.32	1.06	1.00
T/β (K)	250	242	290	310
A_{HK}	77.911	62.380	51.918	34.986

Table 2
The parameters of Eq. (13) for different adsorbates analyzed in the current paper

Parameter	Adsorbate			
	Ar	N_2	CCl_4	C_6H_6
$a_{1(all)}$	0.7864	0.7775	0.8206	0.8951
$b_{1(all)}$	−6.5449	−9.5761	−14.0445	−15.0715
$c_{1(all)}$	2.1878	2.1227	2.5580	2.6875
$a_{2(all)}$	79.6156	53.7290	53.3734	39.7903
$b_{2(all)}$	−27.2554	−13.8278	−18.2474	−14.3832
$c_{2(all)}$	4.0201	1.7692	2.6748	2.1493

$$\frac{L_{av(all)}}{d_A} = \frac{a_{1(all)}}{1 + b_{1(all)}\exp[-c_{1(all)}n]} + \frac{a_{2(all)} + b_{2(all)} \times n + c_{2(all)}n^2}{E_0}, \tag{13}$$

not only for the micropore diameters (called the first range), and [27–32]

$$\frac{L_{av(mic)}}{d_A} = \left(\frac{a_{1(mic)}n}{b_{1(mic)} + n}\right)\left(\frac{a_{2(mic)}n}{b_{2(mic)} + n}\right)^{E_0} \times E_0^{\left(\frac{a_{3(mic)}n}{b_{3(mic)}+n}\right)} \tag{14}$$

for calculations up to effective diameter equal to 2 nm (called the second range). The values of parameters are given in Tables 2 and 3 [7,29–32]. The additional details of all above-mentioned calculations were given previously [7,28–32]; therefore they are omitted in the current study. Taking into account the assumptions made during the derivation of Eq. (12), the main condition, which should be fulfilled for the chosen molecules of adsorbates, is the absence of a dipole moment and a spherical-like structure. Therefore, we chose N_2, Ar, CCl_4, and C_6H_6. For some of these adsorbates the Horvath–Kawazoe method was adopted earlier, for example, for N_2 [42,43], Ar [45] and/or C_6H_6 [46]. Moreover, these adsorbates have been widely applied in the investigation of the structural heterogeneity of microporous carbons. However, the choice of nitrogen at its liquid temperature as the probe molecule may not be suitable for very narrow pores such as those in carbon molecular sieves, where the activated diffusion effects might be important. These effects can be reduced by conducting the experiment at higher temperatures. It is thus useful to investigate the MSD ob-

Table 3
The parameters of Eq. (14) for different adsorbates analyzed in the current paper

Parameter	Adsorbate			
	Ar	N_2	CCl_4	C_6H_6
$a_{1(\mathrm{mic})}$	15.9173	24.1672	11.9839	18.3776
$b_{1(\mathrm{mic})}$	1.5868	2.2709	1.5805	3.2093
$a_{2(\mathrm{mic})}$	0.9839	0.9960	0.9916	1.01
$b_{2(\mathrm{mic})}$	-2×10^{-2}	-1.29×10^{-2}	-1.86×10^{-2}	-8.92×10^{-4}
$a_{3(\mathrm{mic})}$	−0.5259	−0.8586	−0.5657	−1.0718
$b_{3(\mathrm{mic})}$	0.8743	1.2266	0.8047	2.1161

tained from adsorption of different adsorbates at temperature other than the boiling point of nitrogen at ca. 77.5 K, for example at near-ambient temperatures. The temperatures chosen in the calculation were equal or very close to those applied in measurements where the investigated adsorbates are used for the determination of structural heterogeneity of carbons. The temperature was equal to liquid nitrogen temperature for N_2 and Ar adsorption, to room temperature for C_6H_6 and CCl_4 (liquid density at the temperature of measurement was used in the calculation of the parameters in Eq. (12)). These temperatures as well as the final values of constants A_{HK} are given in Table 1 (the other physicochemical constants of the adsorbent and the adsorbates, used in calculations of Eq. (12), and the final values of B_{HK}, C_{HK}, and D_{HK} can be found in [7,29–32]).

Summing up, all the above results show that the average pore diameter is a function not only of E_0 but also of n. Then, using Eqs. (13) and/or (14), the average reduced effective diameter can be calculated and multiplied by the adsorbate diameter (Table 1). The typical plots (the lines) for chosen adsorbates (C_6H_6 and N_2) and values of n (1.50 and 3.25) are compared with relationships proposed by the other authors (points) in Fig. 1. It should be pointed out that the shape of this curves is similar to that observed for the empirical and/or semi-empirical relationships. This procedure was also applied previously [7,29–31,33] to experimental data of adsorption on different carbonaceous molecular sieves. The correlation between suggested and calculated using Eqs. (13) and (14) pore diameters is very good.

On the other hand, we recently tried to answer the most general questions: *What kind of PSD assumes DA equation itself? Does this distribution change if the parameters of the DA isotherm change (especially n)* [35]. A partial answer to this problem has recently been given by Ohba and co-workers [47,48]. They studied the simulated nitrogen adsorption isotherms in heterogeneous carbons and assumed Gaussian distribution of pores. It was shown that the simulated isotherms can be fitted by typical DR, although not in the whole range of relative pressures. The interesting approach of Ohba and co-workers [47,48] was extended [35], and the problem was investigated from the opposite point of view. Two groups of low-temperature ($T = 77.5$ K) N_2 adsorption isotherms were generated [35]. We studied the influence of n at constant E_0 and, to the contrary, the effect of E_0 at constant n. The obtained curves were converted into high-resolution α_s-plots in order to explain the mechanism of adsorption. Moreover, the new algorithm (called the adsorption stochastic algorithm (ASA)) [49–53] was used to solve the problem of fitting the local adsorption isotherms of the Nguyen and Do method [51,54–56] to experimental data [49–56]. The obtained results show that the DA equation generates isotherms describing almost a homogeneous structure of pores and/or a bimodal heterogeneous structure [35]. Corresponding PSDs indicate the presence of homogeneous porosity, primary and/or secondary micropore filling, or both. The parameter n of the DA equation is responsible not only for the homogeneity of pores (i.e., the deviation of pores from average size) but for the adsorption mechanism in micropores. In other words, lowering n leads to the change in this mechanism from primary to simultaneous primary and secondary micropore filling. Taking all obtained results into account suggests that the DA equation is probably the most universal description of adsorption in micropores.

All theoretical models (as, for example, considered in the current study: HK, ND, and DFT) are connected with their own specific assumptions of the description of the porous structure and/or mechanism of adsorption. Of course, those postulations can significantly influence obtained results, i.e., PSD curves. The modeling of local and/or global adsorption isotherms for different pore widths using DFT theory, Monte Carlo simulations, and the ND model leads to results that should be, for some cases, treated with caution. The main simplifications of those theories are, for example, the neglect of the pore connectivity, ignoring of different thickness of carbon microcrystallites forming micropores, or existence of various surface groups on the surface of activated carbons. Moreover, it is very difficult to find papers where authors obtained satisfactory results (using the above-mentioned theories) describing simultaneously the experimental adsorption isotherm, adsorption enthalpy, and entropy (or heat capacity) for adsorption in microporous carbons around room temperature. Although all simulation and modeling of carbons is very interesting and sometimes spectacular [57–63], it should be remembered that small changes in the values of fundamental parameters taken as constants in calculations can lead to drastic changes in the results obtained, as shown in the important papers by McEnaney and co-workers

[64] and others [65,66]. In our opinion the results of this type of the calculation are speculative as long as a satisfactory model of the structure of carbons is not evaluated. It should be pointed out that very complicated models of the structure of a microporous activated carbon are sometimes considered in some advanced numerical and simulation calculations (for example, the RMC method, where the surface sites have been added at random points on the edges of the graphene microcrystals characterizing by differing size and shape [60]) in order to describe the "real" structure of activated carbons. However, taking into account this complex structure is connected with considerable extension of the time of calculations. On the other hand, very puzzling results are obtained from the description of the micropore structure of various carbonaceous materials (the different origin and thermal (or chemical) treatment)) for the reason that the differences between the micropore size distribution plots are insignificant. For example, Ismadji and Bhatia published the results of microporosity determination from DFT method for three carbons, Filtrasorb-400, Norit ROW 0.8, and Norit ROX 0.8 (Fig. 3 [67] and/or Fig. 2 [68]). The number of peaks on PSD curves and the ranges of their location, as well as the shapes, are very similar. The same situation occurs often for other carbons (for example, the DFT method leads to very similar results for carbon D43/1 (Carbo-Tech, Essen, Germany) as for carbons WD and AHD (Hajnówka, Poland) (Fig. 11 [52])). In our opinion this behavior of PSDs is very surprising and can be caused by the low sensitivity and the simplifications of the mentioned above methods.

On the other hand, the most important limitations of the Horvath–Kawazoe model (this method is the leading subject of our current study) are widely described, for example by Dombrowski and co-workers [69] and Rege and Yang [70]. The main restrictions are the following: the overestimation of the filling pressures relative to DFT and molecular simulation results, incorrect adsorbate pair interaction, "unstructured" local density profiles, assuming one-stage micropore filling, and equating the free-energy change upon adsorption to the average interaction energy of the adsorbing molecules. Summing up, the HK method and the potential theory of adsorption have limitations, although they are very popular. Their foundation are questionable on the basis of theoretical studies involving density functional theory calculations and computer simulations [59]. There are attempts to improve the HK method and success was achieved in improving the relation between the pore width and equilibrium pressure [25,38,69–72]. Surprising results were recently observed by Jaroniec and co-workers [73]. They showed that the HK method can be successfully used for the characterization of ordered mesoporous silicas and related materials. Moreover, some authors stated that the HK and DFT methods of pore size distribution determination lead to very similar results [7,30,31,72,74], and that confirms the validity of the assumptions of the HK method as well as its applicability to the determination of microporosity of carbons. On the other hand, others suggested that the HK method is not effective for highly microporous carbons and a further improvement of this method is required [62,75–77]. In our opinion, the results of the scientific reports lead to the statement that for some microporous carbons the similarity between both methods exists. Valladares and co-workers [59],

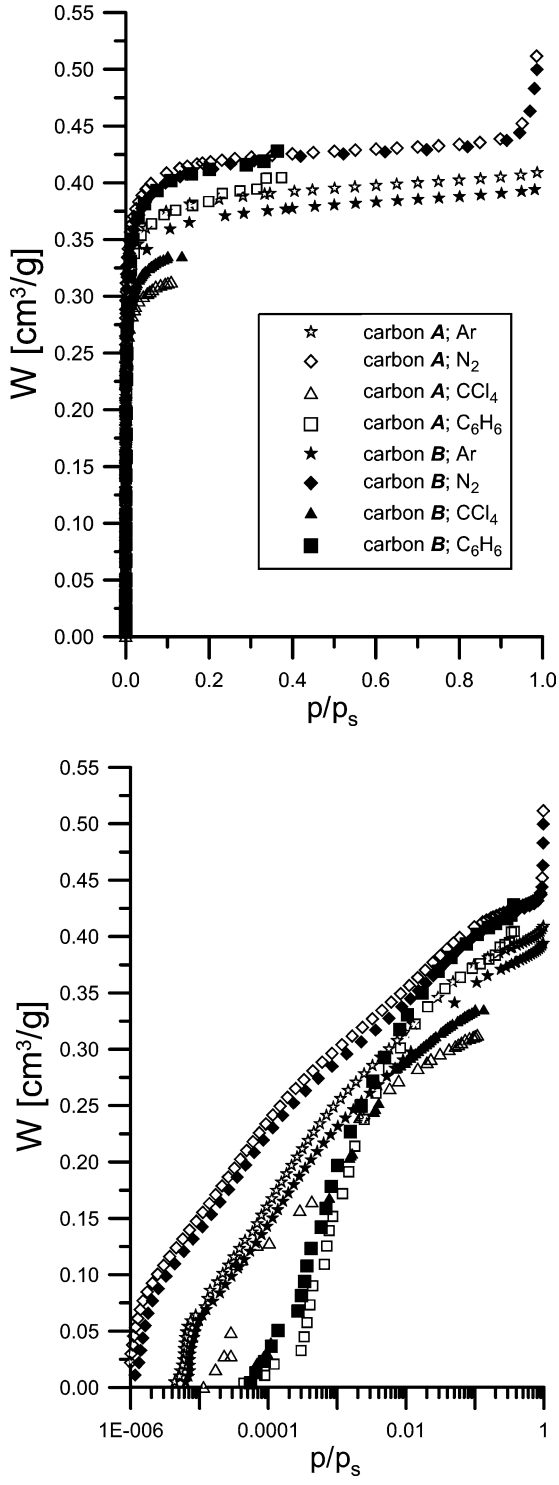

Fig. 2. Adsorption isotherms of Ar, N_2, CCl_4, and C_6H_6 on activated carbon: A (open symbols) and B (closed symbols).

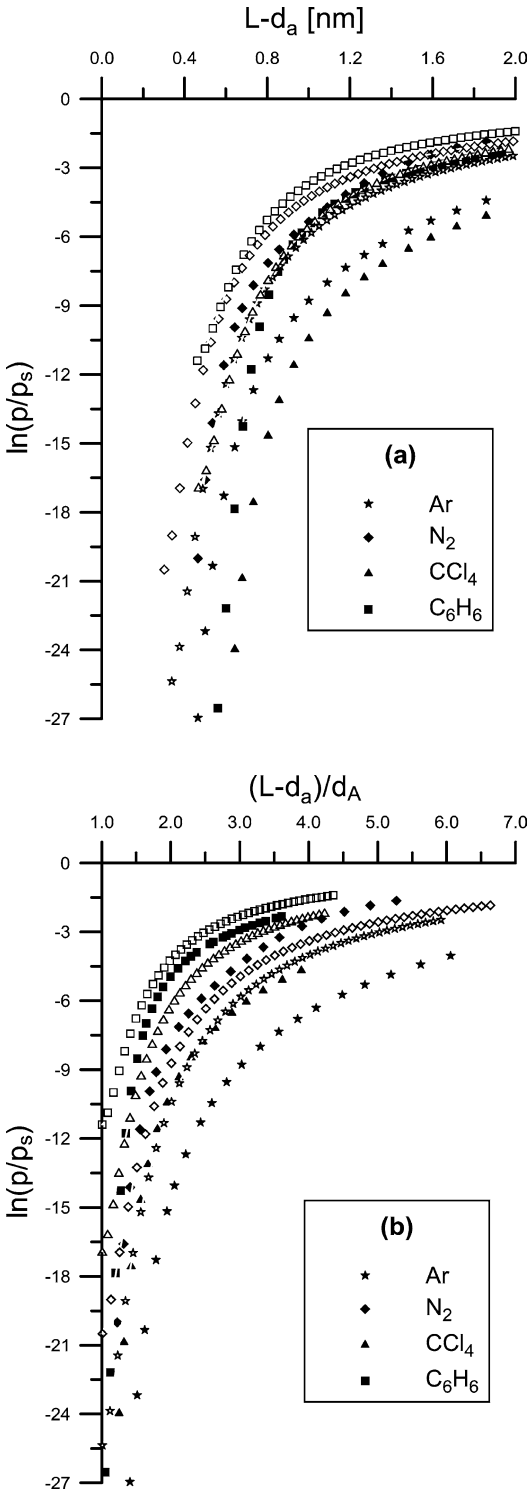

Fig. 3. (a) The general relationships between effective pore diameter $(L - d_a)$ and relative pressure (p/p_s) for adsorption of four analyzed adsorbates; open symbols—the Horvath and Kawazoe theory; closed ones—the Nguyen and Do method (for CCl_4 the following parameters were adopted: $\sigma_{ff} = 0.3305$ (nm) [85]; $\varepsilon_{ff} = 118.05$ (K) [85]; $\gamma = 0.0132$ (N/m) [97]; $\nu = 2.727 \times 10^{-5}$ (m^3/mol) [98]; $C_{BET} = 97.80$ [99] and for Ar: $\sigma_{ff} = 0.5140$ (nm) [100]; $\varepsilon_{ff} = 366.00$ (K) [100]; $\gamma = 0.02488$ (N/m) [97]; $\nu = 9.830 \times 10^{-5}$ (m^3/mol) [98]; $C_{BET} = 59.32$ [101]. (b) The influence of adsorbate size (diameter, d_A) on the plots presented in Fig. 3a. The pore-width is replaced by "reduced" effective variables $((L - d_a)/d_A)$.

based on molecular simulation methods, showed, that the validity of the results of HK method depends on the micropore structure of studied carbon. More reliable results (comparing to DFT) are obtained for strictly microporous adsorbents [7,30,31].

Therefore, it can be concluded that systematic investigation of the pore structure of the wide class of adsorbents characterized by the various type of heterogeneity is necessary. Nine microporous carbon films obtained from cellulose by Zawadzki and co-workers [78] (and next chemically modified) were investigated previously to evaluate their porosity [30]. Similarity was observed between the results obtained by the DFT and HK methods, and this confirms the results of Valladares et al. [59]. It was concluded that a good correlation occurs between the pore diameters obtained from DFT analysis (for N_2 adsorption), those calculated from C_6H_6 calorimetry data using the Everett and Powl potential [44], and those calculated applying the recently developed equation (Eqs. (13) and (14)). The final results show that in the structure of these adsorbents the majority of micropores possess the same diameter (a very narrow distribution of pores). Summing up, past studies [30] were limited to adsorption of nitrogen (77.5 K—nine samples altogether) and benzene (313 K—for one sample the isotherm and adsorption enthalpy was measured) on microporous carbons with homogeneous porosity where the "primary micropore filling" occurs. In our opinion, the Horvath and Kawazoe method is very simple, and therefore it can be applied in the current study as a useful tool to show different aspects connected with the important and complicated problem of the characterization of porosity.

The next unsolved problem (due to the difference in results met in the literature—for example [79–85]) of the characterization of the heterogeneous pore structure of solids (carbonaceous materials, especially) is the analysis based on the isotherms of several simple adsorbates. Jagiełło and Schwarz [79] stated that for the series of different adsorbates and the same adsorbent (activated carbon G210 and/or molecular sieving carbon MSC-5A) "it is seen that except for CO_2 all other adsorbates (N_2, CH_4, C_2H_4, and C_2H_6) give practically overlapping functions MSDs." This difference was explained by these authors in the following way—the CO_2 molecule has to be "thinner" than other considered molecules. Wang and Do [80], for characterization of the micropore-size distribution of activated carbons (Ajax and/or Nuxit), presented an approach using simultaneous theoretical description of multiple-temperature (three or four for the individual adsorbent) experimental isotherm data of many adsorbates (eight for the individual adsorbate; for example, for Ajax activated carbon, methane, ethane, propane, butane, benzene, toluene, carbon dioxide, and sulfur dioxide). In this case the MSD is treated as an intrinsic property of the activated carbon (independent of an adsorbate) and the sole source of heterogeneity in spite of different adsorbates having access to different pore size ranges (different

molecular sizes). On the other hand, in the same situation as considered above, some authors observed significant differences in MSDs—for example, Jagiełło and Schwarz [79], who compared the micropore-size distribution of two carbons (G and/or M) calculated from CF_4 and SF_6 adsorption data. The differences between micropore size distributions were also reported by Trznadel and Świątkowski (Horvath–Kawazoe method; adsorbates: N_2, Ar, and C_6H_6; adsorbent: granulated A-type activated carbon [81]), Dombrowski and co-workers (DFT method; adsorbates: N_2 and Ar, adsorbent: two activated carbons, Saran and/or coconut char [82]), Nguyen and Do (adsorbates: N_2, C_6H_6 (three temperatures), adsorbent: Ajax and/or ACF [83]). We agree with the point of view of Nguyen and Do, who try to explain these discrepancies in the following way: "(they are caused by) difference in the experimental temperatures and molecular properties, such as molecular dimension, molecule–molecule interaction energy, etc." Interesting results were presented by Scaife and co-workers [84]. A set of measurements of gas adsorption (nitrogen (77 K), methane (293.1 K), argon (77 K), and carbon dioxide (293.1 K)) of a single sample of AX21 were investigated based on DFT. Scaife and co-workers found, for example, that the pore structures predicted for AX21 using nitrogen at 77 K and carbon dioxide at 293.1 K are quite different, CO_2 showing a unimodal micropore peak not seen at 77 K by nitrogen or argon. Moreover, the PSD for carbon dioxide was shifted to smaller pores compared with other adsorbates. On the basis of those studies they recommended CO_2 as the adsorbate for characterizing the pore structure of carbonaceous adsorbents (is a more accurate probe of micropore structure than nitrogen at 77 K). Moreover, they suggested that the change of apparent PSD could be monitored by performing a series of isotherm measurements form high (equal and higher than room temperature) to low temperatures. It is very important that Scaife and co-workers [84] stated that the accuracy of the PSD could be improved by fitting to isosteric enthalpies as well as the adsorption isotherm. Ravikovitch et al. [85] presented an approach to PSD characterization of microporous carbonaceous materials such as activated carbon and carbon fibers based on nonlocal DFT for nitrogen, argon, and carbon dioxide adsorption at standard temperatures (77 K (N_2 and Ar) and 273 K (CO_2)). The authors suggested that frequently observed disagreement between PSDs obtained from adsorption isotherms of different gases and those measured at different temperatures was mostly attributed to the shortcomings of the slit-like pore model, in particular to the molecular sieving and networking effects and specific adsorbate–adsorbent interactions. However, Ravikovitch and co-workers [85] believe that possible inconsistencies in the pore size distributions calculated from different isotherms may be caused by the choice of the parameters for intermolecular interactions and also by the solution of the ill-posed problem of deconvolution of the integral adsorption equation. They always observed (for all analyzed adsorbents) a good agreement between nitrogen and argon distributions. PSD curves calculated from carbon dioxide isotherms were in good agreement with those evaluated for the above-mentioned adsorbates only for ultramicropores and micropores narrower than ca. 1 nm.

Summing up, the results presented in this section lead to the statement that for microporous carbons the extensive investigation should be still continued. Therefore, in the present paper we try to extend the analysis on the adsorption on two strictly microporous activated carbons with wider dispersion of pores (i.e., being more heterogeneous) comparing with the mentioned carbonaceous films [30]. Moreover, the influence of the diameter of adsorbates (d_A) and the temperature (T) of the adsorption measurements is analyzed in order to explain the differences between calculated values of the average diameters (L_{av}) and the plots of the micropore-size distributions (MSDs) determined from adsorption data of different adsorbates. The results of the HK method [42,43] are compared with those from the Nguyen–Do and DFT methods (they are treated as the reference methods) [53,54,86], from adsorption calorimetry [87–90], and from the method proposed by Everett and Powl [44].

2. Experimental

The adsorption sieving properties of two ashless microporous polymeric carbons (called A and B) obtained from polyfurfuryl alcohol [87,88,91,92] are investigated in this study. The initial carbon (A) with a negligibly small concentration of oxygen functionalities, was oxidized with nitric conc. acid at 353 K for 2 h (carbon B). The detailed procedure of carbon preparation and the carbon surface characteristics were given previously [87,88,91,92].

Nitrogen and argon adsorption isotherms at 77.5 K, presented in this paper, were determined using the ASAP 2010 MicroPore System (Micromeritics, Norcross, GA, USA), an automatic volumetric adsorption apparatus. Both carbons were desorbed for three hours in a flow of He, carbon A at 573 K, and carbon B at 493 K (a constant pressure of ca. 10^{-5} Pa was obtained). Benzene adsorption isotherms (and the corresponding enthalpy of adsorption) were measured on carbons A and B at the temperature of 313 K (for carbon tetrachloride the measurements were performed at 308 K). Isotherms were determined using the volumetric apparatus described by Kiselev and Dreving [89] with Baratron pressure transducers (MKS Instruments, Germany). The differential enthalpy of adsorption was determined using a Tian–Calvet microcalorimeter described previously [87,88,91,92]. During the calculation the values of liquid density (ρ) and the pressure of saturation (p_s) collected in Table 1 were applied. The comparison of the experimental adsorption isotherm data is given in Fig. 2.

3. Results and discussion

3.1. The influence of the temperature and the adsorbate diameter on the micropore-size distributions—the HK method

The starting point of our current consideration are the results of the calculation of the relative pressure (p/p_s) versus micropore effective width ($L - d_a$) for Ar, N_2, CCl_4, and C_6H_6 based on Eq. (12) and values of parameter A_{HK} collected in Table 1 and $B_{HK} - D_{HK}$ taken from [7,29–32]. In order to determine the pore-size distribution, the new DHK (determining Horvath–Kawazoe) procedure described recently [33,34] was applied. The standard bisection procedure is used as a kernel in the proposed algorithm. This method gives stable results for most of non-linear functions and the computation takes a very short period of time (short range of changes in the micropore widths, which are determined). Fig. 3a (open symbols) shows the final theoretical results of the calculations obtained for adsorption of analyzed adsorbates in slit-like pores [32–34]. The maximum value of the effective pore-width on Figs. 3–5 is restricted to 2 nm in order to provide the readers with some nuances of the analyzed plots. Moreover, this value is the upper limit of micropore diameters recommended by IUPAC [93]. As shown in Fig. 3a, the relative location of ($L - d_a$) vs (p/p_s) is connected with the type of adsorbate, but all curves presented in this figure have the same shape. It can be noticed that the adsorbates fill the pores with arbitrarily chosen diameter (with increasing relative pressure values) in the following order: Ar, CCl_4, N_2, and C_6H_6. This sequence does not depend on the parameter A_{HK} of the master equation (Eq. (12)). The curves for Ar and CCl_4 as well as N_2 and C_6H_6 converge for the finer range of micropore dimensions. On the other hand, for CCl_4 and N_2 the curves coincide for pore widths close to 2 nm, as can be seen in Fig. 3a. For the wider pores than presented in this figure (mesopores) these plots predict similar values of the relative pressure (increasing to unity) as obtained from the Kelvin equation, the BJH method, DFT simulation, Gibbs ensemble Monte Carlo molecular simulation, and other methods [54,57,69,94,95].

It is obvious that the values of the physicochemical parameters can influence the obtained curves of ($L - d_a$) vs (p/p_s) presented in Fig. 3a. It is very difficult unambiguous state at the moment which the parameters have a decisive effect on the obtained results because the parameters $A_{HK} - D_{HK}$ (Eq. (12)) are the functions of many variables. Each atom or molecule of the adsorbates considered here is characterized by the different diameter, d_A (Table 1) and therefore they possess different accessibility to the micropore structure of the analyzed adsorbents. It seems very probable that d_A has a significant influence on the results presented in Fig. 3. To take the type of adsorbate into account these plots are converted into "reduced" effective width plots of the function $\ln(p/p_s) = f((L - d_a)/d_A)$—Fig. 3b (open symbols). This recalculation (application of the reduced variable) standardizes the description of the adsorption process and it will be used a few times in the current paper. As a result, the shape of the analyzed curves does not change but this figure is more legible. The effect of temperature on the filling pressure of pores can also be observed in

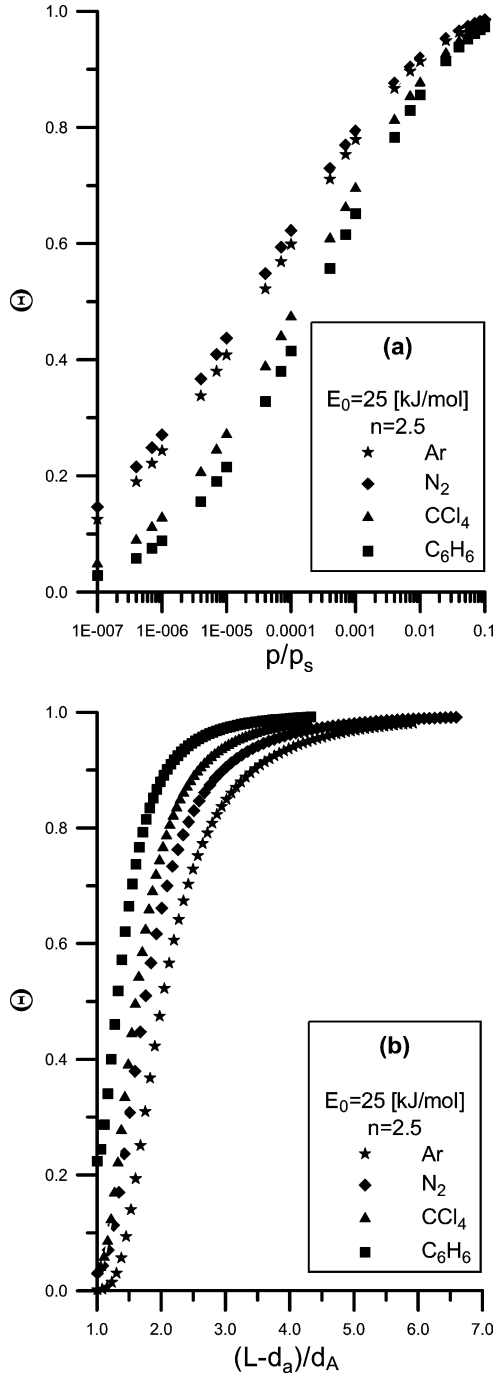

Fig. 4. (a) The influence of the type of adsorbate on the adsorption isotherms generated based on the Dubinin–Astakhov equation (Eq. (1)) applying the parameters (β and T) collected in Table 1. (b) The comparison of the relationships Θ vs ($(L - d_a)/d_A$) for all analyzed adsorbates (only the HK model is analyzed). Plots are obtained from the data presented in Figs. 3b and 4a.

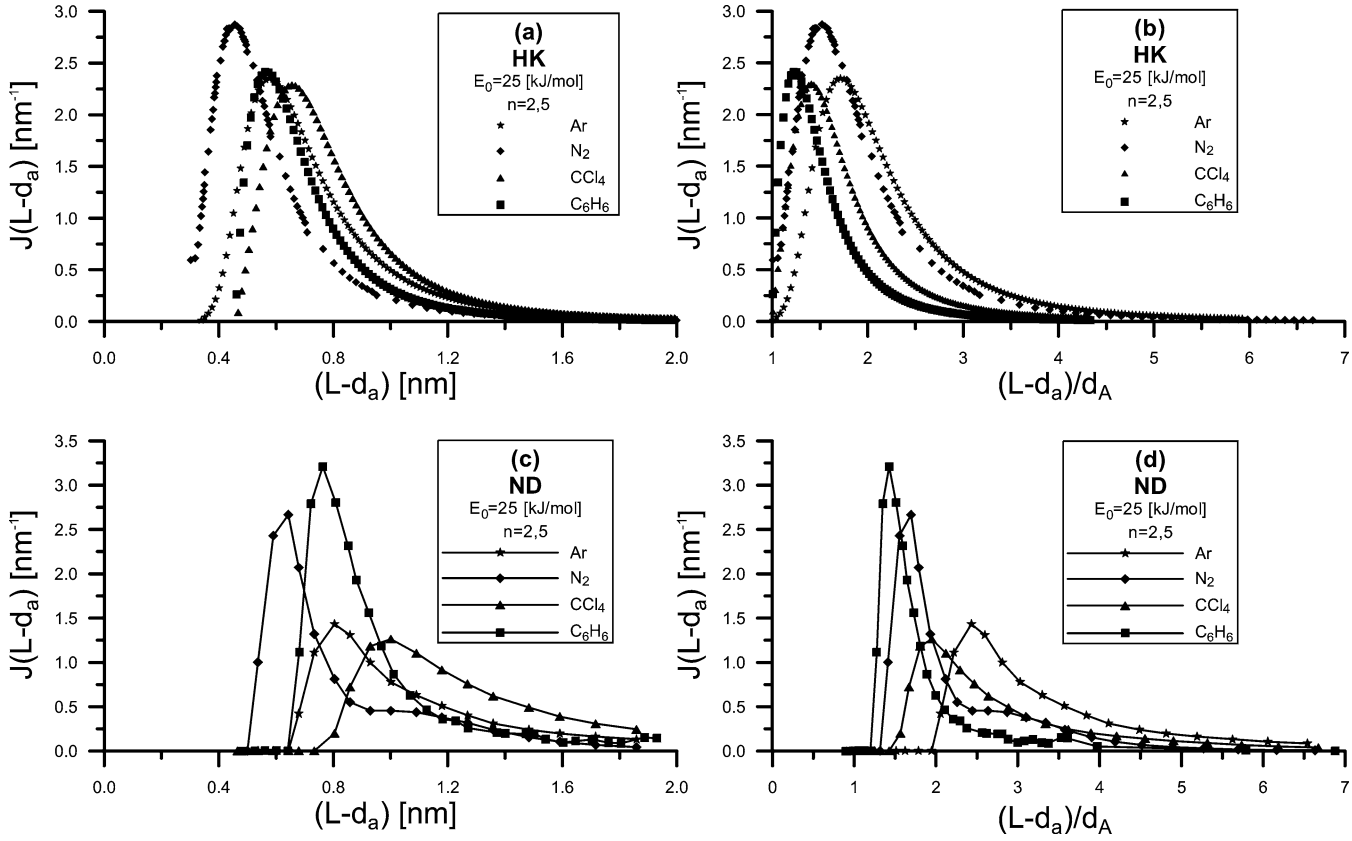

Fig. 5. The influence of the type of adsorbate on the micropore size-distribution plotted as a function of the effective micropore width (or the reduced effective micropore width) for characteristic energy, E_0, equal to 25 kJ/mol and parameter of the DA equation $n = 2.5$, based on the HK and ND models, respectively.

this figure. In general, for a pore of a given ($(L - d_a)/d_A$), the lower the temperature (Ar and N_2), the sooner pore filling occurs (in terms of relative pressure). In contrast to data presented in Fig. 3a, here, the sequence of adsorbates for fixed reduced pore widths is Ar, N_2, CCl_4, and C_6H_6 and it is the same as obtained for the parameter A_{HK} (Table 1) of the master equation (Eq. (12)). Furthermore, in this situation the curves do not coincide in the low range of the reduced slit-widths, but for wider pores, as can be observed for data presented in Fig. 3a.

In the next figure (Fig. 4a) the influence of the type of adsorbate on the adsorption isotherms generated based on the Dubinin–Astakhov equation (Eq. (1)) is shown (during the calculation the values of β and T collected in Table 1 were applied). Adsorption isotherms are presented in this figure at relative pressure from 1×10^{-11} up to 1 p/p_s and they are generated for arbitrarily chosen values of the characteristic energy of adsorption (the same for all analyzed adsorbates), $E_0 = 25$ kJ/mol, and the exponent of the DA equation, $n = 2.5$ (obviously the assumption of the same E_0 value for all the adsorbates simplified the considerations—the influence of the temperature and the affinity coefficient is emphasized). All generated isotherms, shown in Fig. 4a, belong to 1st type of IUPAC classification [93] (i.e., Langmuir-type) as it is also observed for experimental data shown in Fig. 2. As it turned out, the ratio of the temperature to the affinity coefficient, T/β has the main influence of plots presented in this figure (the same values of E_0 and n). In order to explain this situation the Dubinin–Astakhov equation (Eq. (1)) is converted to the following form:

$$\Theta = \exp\left[-\left(\frac{A_{\text{pot}}}{\beta E_0}\right)^n\right] = \exp\left[-\left(\frac{T}{\beta}\right)^n\left(\frac{R\ln(p_s/p)}{E_0}\right)^n\right]. \tag{15}$$

The values of the ratio (T/β) are shown in Table 1—the highest one is obtained for C_6H_6 (310 K) and the lowest for N_2 (242 K). A general tendency in Fig. 4a is that for a fixed value of the degree of pore filling (Θ), p/p_s decreases with (T/β). In the other words, for two microporous solids with different values of analyzed ratio, the same fraction of filled micropores occurs at a lower value of p/p_s for a solid with a higher ratio of temperature to the affinity coefficient. Thus, in this situation the location of curves is determined again by the parameter characterizing adsorbate and the temperature of the adsorption process.

In order to obtain the differential micropore-size distribution, the relationship between the adsorption, W (or relative adsorption, $\Theta = (W/W_0)$) and arbitrarily chosen parameter characterizing the micropore size, should be known. In the current paper, micropore size distributions are evaluated based on $(J(L - d_a) = d\Theta/d(L - d_a))$. For example, knowing the adsorption isotherm data (Θ vs p/p_s—

Fig. 4a) and assuming the relationship between the relative pressure and pore width (Fig. 3b), the wanted function $\Theta = f(L - d_a)$ is very easy to obtain. Thus, the comparison of relationships Θ vs $((L - d_a)/d_A)$ for all analyzed adsorbates is shown in Fig. 4b based on the results presented in Figs. 3b and 4a. The main conclusion drawn from the results shown in this figure is the decisive effect of function the $(\ln(p/p_s) = f((L - d_a)/d_A))$ on the calculated MSDs while the fixed values of E_0 and n are assumed. In the other words, the shape of MSDs characterized by the maximum value of function $J(L - d_a)$ related to $(L - d_a)_{p,\max}$ (or $((L - d_a)/d_A)_{p,\max}$), is determined to a larger extent by $(\ln(p/p_s) = f((L - d_a)/d_A))$ than by $(\Theta = f((L - d_a)/d_A))$ due to similarity of the sequences of curves observed in Figs. 3b and 4b. The sequence of the value of $((L - d_a)/d_A)_{p,\max}$ related to the maximum value of $J(L - d_a)$ for the various adsorbates (Figs. 5a and 5b) is the same as the sequence of curves presented in Figs. 5c and 5d.

The influence of the type of adsorbate on the differential micropore size distribution, plotted as a function of the effective and reduced effective micropore width, for the values of the characteristic energy E_0, equal to 25 kJ/mol and parameter of the DA equation, $n = 2.5$ are shown in Figs. 5a and 5b. A simple numerical differentiation procedure is used [31,33,34,53,96]. The MSD plots are the asymmetrical bell-shaped function possessing two points of inflexion.

In order to achieve the same PSDs $(J(L - d_a) = d\Theta/d(L - d_a))$ for different adsorbates the identical plots of the relationship between the degree of micropore filling vs effective pore diameter (or pore diameter) should exist. According to Eqs. (1) and (12), each isotherm can be presented as the function $\Theta = f(L)$ (see also Fig. 4b). Next, the derivative can easily be calculated numerically. Therefore, the low-temperature nitrogen adsorption isotherms were generated at relative pressures from 1×10^{-7} up to 1 for arbitrarily chosen values of both parameters of the DA equation (i.e., the first set ($E_0 = 24.86$ kJ/mol and exponent $n = 2.54$) and the second one ($E_0 = 24.41$ kJ/mol and exponent $n = 2.39$)). Summing up, these parameters are obtained from the fitting of the theoretical model (Eq. (1)) to the experimental N_2 isotherms for carbon A and B, respectively (investigated in the current study (see Fig. 2 and Table 1)). These data are treated as the reference. In order to obtain the values of the characteristic energy and exponent of the DA equation for the remaining three adsorbates, the nonlinear fitting procedure is used again. The goodness of the fit of the theoretical model (Eqs. (1) and (12)) for Ar, CCl_4, and C_6H_6 to the reference N_2 adsorption data is expressed by the determination coefficient (DC). The following results are obtained: for carbon A, Ar ($E_0 = 36.76$ kJ/mol, $n = 2.46$, and DC = 0.9999), CCl_4 ($E_0 = 42.11$ kJ/mol, $n = 2.58$, and DC = 0.9938), and C_6H_6 ($E_0 = 30.43$ kJ/mol, $n = 2.50$, and DC = 0.9963); for carbon B, Ar ($E_0 = 36.07$ kJ/mol, $n = 2.31$, and DC = 0.9999), CCl_4 ($E_0 = 41.48$ kJ/mol, $n = 2.38$, and DC = 0.9944), and C_6H_6 ($E_0 = 29.94$ kJ/mol, $n = 2.32$, and DC = 0.9967). The final conclusions and the comparison with the experimental data will be given below.

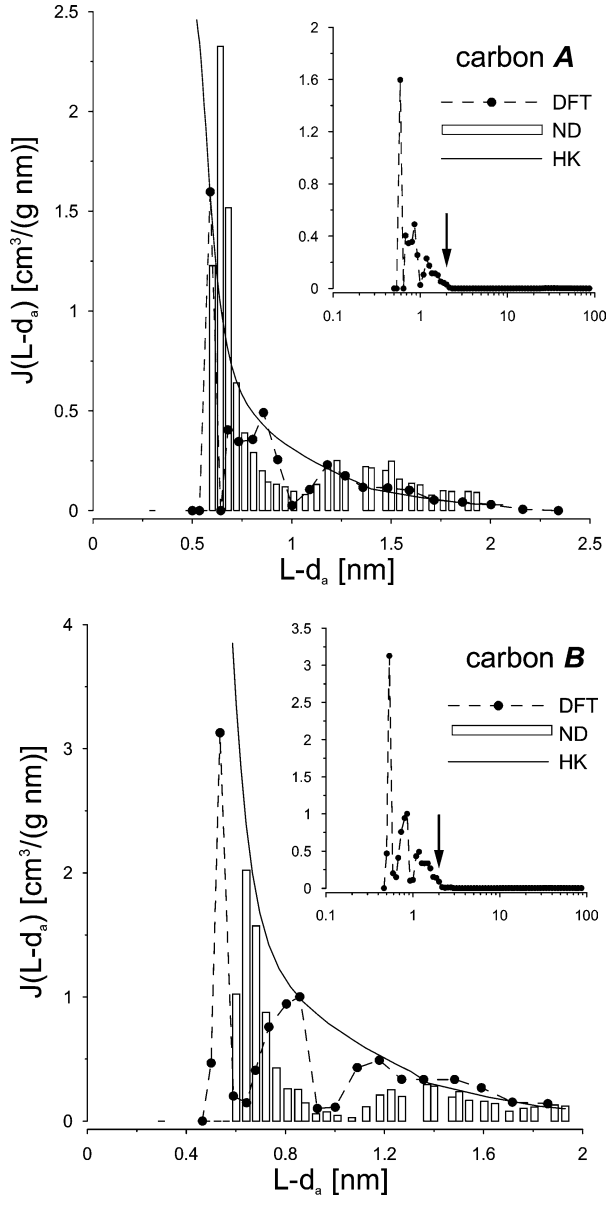

Fig. 6. Pore size distributions for studied activated carbons obtained on the basis of the Nguyen and Do method, DFT theory, and the Horvath and Kawazoe method (only the range of micropores is shown). Additionally the total pore-size distribution from DFT method is presented a second time separately in the smaller figures—the arrow denotes the upper limit of the widths of micropores.

3.2. The influence of the temperature and the adsorbate diameter on the micropore-size distributions—the ND method with the ASA algorithm

In Fig. 3 we also show a comparison of the so-called master curves (i.e., pore filling pressure, p/p_s, vs effective pore diameter, $(L - d_a)$, or "reduced" effective pore diame-

ter, $(L - d_a)/d_A)$), generated from the Nguyen–Do (with the previously proposed adsorption stochastic algorithm (ASA) for the solution of linear Fredholm integral equation of the first kind [53]). It should be pointed out that the ND method was shown to be applicable for determination of porosity of carbonaceous materials, and as shown previously, leads to practically the same results as the DFT method [50,51]. In the current paper this method is adopted probably for the first time for adsorption data of CCl_4. For other adsorbates the parameters can be found elsewhere [54,95]. It is very important that Figs. 3a and 3b show that similar sequences of pore filling pressure vs effective pore diameter curves obtained from ND and HK methods, and the shift of the results of the ND method to larger pore diameters is observed. The only difference is for the curves shown in Fig. 3a for N_2 and CCl_4, and this is caused by the differences in molecular diameters taken for calculations in the both methods (it should be stated that idea of the values of particular parameters is treated optionally and freely by some authors and, unfortunately, one can find different values of the same parameter in the literature).

Fig. 5 shows the pore size distributions obtained from the ND method for the same values of parameters of DA equation as for analysis of the HK model (the results presented in the same figure). The pore-size distributions calculated form the Nguyen–Do method shift to larger pore diameters in comparison with the HK model (and this is caused by the difference of the pore filling pressure vs pore diameter curves shown in Fig. 3). However, similar sequences of curve connected with both types of theories is observed.

3.3. The experimental verification of theoretical considerations

3.3.1. Pore size distributions—the low-temperature nitrogen adsorption data analysis

Based on the results of low-temperature nitrogen adsorption isotherms (they are shown among other things in Fig. 2) the structure of carbons A and B was characterized using different methods (the obtained results are collected in Table 4). Some of them were applied previously for the characterization of carbonaceous films [30]. Therefore, they are not described in the current studies and the detailed description can be found in [30]. However, the meaning of parameters is presented in Appendix A.

We have recently underlined [30,53,74] that there is a problem connected with the comparative analysis of the results of DFT method with those obtained from the other ones, especially from the methods based on DR and/or DA equation. The reason is that the empirical equations proposed for the calculation of the average micropore diameters correlate the characteristic energy of adsorption, obtained mainly from DR equation (see below) with the average width of the slit. The best fit of DR and/or DA equation to experimental data of adsorption, discussed in the current study, was obtained for the data measured up to the relative pressure ca. 0.1 (Table 5). There are the following reasons of this choice. The percentage contribution of the volume of micropores evaluated from DA or DR equations ($(W_{0DA/0DR})$, divided by the maximum value of adsorption of nitrogen (at $p/p_s \approx 1$)) are similar to those calculated from the DFT method ((the total volume of the micropores with diameters smaller and/or equal to 2 nm, V_{DFT}^{micro}), divided by the total volume of micropores determined from the upper value of the cumulative pore size distribution, V_{DFT})—see the results collected in Table 4. On the other hand, the comparison of the values of the ratio of the volume of the primary micropores to the total pore volumes determined from DFT ($V_{DFT,I}^{micro}/V_{DFT,tot}$) with those calculated from the potential theory equations (the Dubinin–Astakhov (DA) (Eq. (1)) and/or Dubinin–Radushkevich (DR) (Eq. (1), $n = 2$)), leads the statement that the same values are obtained if the adsorption isotherms are analyzed by this theory in the range lower

Table 4
Structural data of two carbons, A and B (nitrogen was applied as an adsorbate)—the meaning of parameters are presented in Appendix A

Carbon	A	B
	Surface areas (m^2/g)	
S_{BET}	823.9	852.3
S_{DR}	987.9	914.5
S_{DA}	882.7	823.3
S_{DFT}^{micro}	697.9	907.6
S_{DFT}^{meso}	5.2	9.8
S_{DFT}	703.1	917.4
$S_{c,\alpha}$	994.5	958.0
$S_{me,\alpha}$	24.4	21.9
	Pore volumes (cm^3/g)	
W_{0DR}	0.426 (83.3%)[a]	0.404 (79.0%)[a]
W_{0DA}	0.416 (81.3%)[a]	0.413 (82.6%)[a]
$V_{DFT,I}^{micro}$	0.190 (51.2%)[b]	0.248 (59.2%)[b]
V_{DFT}^{micro}	0.290 (78.2%)[b]	0.340 (81.1%)[b]
V_{DFT}^{meso}	0.081	0.078
V_{DFT}	0.371	0.419
V_{HK}	0.416	0.408
$V_{mi,\alpha}$	0.408	0.408
	Micropore average diameters (nm)[c]	
$L_{av,DFT,I}$ ($L <\sim 1$)	0.702	0.652
$L_{av,DFT,II}$ ($\sim 1 < L <\sim 2$)	1.371	1.362
$L_{av,DFT,tot}$ ($L <\sim 2$)	0.848	0.846
$L_{av,ND,I}$ ($L <\sim 1$)	0.690	0.674
$L_{av,ND,II}$ ($\sim 1 < L <\sim 2$)	1.454	1.516
$L_{av,ND,tot}$ ($L <\sim 2$)	0.890	0.923

[a] For the total micropore volume $W_{0DR/0DA}$ (Dubinin–Astakhov (DA) (Eq. (1) and/or Dubinin–Radushkevich (DR) (Eq. (1), $n = 2$) equations) the percentage contributions are evaluated for the reference—the maximum nitrogen adsorption at $p/p_s \approx 1$.

[b] The same procedure as for the potential theory is applied for the DFT method (in this case the reference is the total volume of micropores determined from the largest value of the cumulative pore size distribution).

[c] The average pore diameters obtained for three groups of micropores (($L <\sim 1$); ($\sim 1 < L <\sim 2$); and ($L <\sim 2$)) based on $J(L - d_a)_{DFT}$ and $J(L - d_a)_{ND}$.

Table 5
Parameters of the Dubinin–Astakhov (DA) (Eq. (1)) and the Dubinin–Radushkevich (DA) (Eq. (1), $n = 2$) equations

Carbon	DA—Eq. (1)				DR—Eq. (1), $n = 2$		
	E_{0DA} (kJ/mol)	n_{DA}	W_{0DA} (cm^3/g)	DC_{DA}	E_{0DR} (kJ/mol)	W_{0DR} (cm^3/g)	DC_{DR}
				Ar			
A	18.91	3.065	0.357	0.9941	17.64	0.419	0.9743
B	18.39	2.698	0.347	0.9941	17.50	0.391	0.9840
				N_2			
A	24.86	2.535	0.401	0.9941	24.48	0.426	0.9883
B	24.41	2.386	0.395	0.9931	24.22	0.413	0.9903
				CCl_4			
A	21.94	2.335	0.323	0.9862	22.14	0.335	0.9829
B	16.80	4.583	0.324	0.9854	18.93	0.370	0.9170
				C_6H_6			
A	18.32	4.823	0.364	0.9947	16.39	0.468	0.9260
B	19.08	4.122	0.390	0.9958	16.98	0.496	0.9461

Note. These equations were fitted to the range of adsorption which takes place in the pores where micropore filling and cooperative swings mechanism occurs (relative pressure less than 0.1 p/p_s); i.e., all micropores were considered).

than 0.002 p/p_s. In the case of adsorption in practically homogeneous microporous structure (as for studied earlier carbonaceous films [30]) the contribution of the volume of primary micropores $V_{DFT,I}^{micro}$ was almost the same as for $W_{0DR/0DA}$. Therefore, the homogeneity of the pore structure is the key factor and following the mechanism of multistage micropore filling published by Kakei and co-workers [102], in the studied carbons the primary and secondary micropore filling occur in the range up to ca. 0.1 p/p_s of the adsorption isotherm. This means that the average micropore diameters, obtained using E_0 values calculated for those ranges of adsorption isotherms, characterize the adsorption process occurring only in the part of the micropores present in the system. Therefore, it should be emphasized that for heterogeneous microporous structures (as occurring in the studied carbons) the values of the pore diameters calculated on the basis of this fragment of the isotherm should be compared only with the total average pore diameters calculated using the density functional method or other advanced numerical methods. Summing up, the average micropore diameters were calculated using the results of the most wide spread equations shown above (Eqs. (2)–(11), (13) and (14)). In order to compare these results, the average pore diameters were calculated for the groups of micropores $L <\sim 1.0$, $\sim 1.0 < L <\sim 2.0$, and $L <\sim 2.0$, based on the numerical integration of cumulative pore size distributions (both DFT and ND models are analyzed).

Table 4 shows that, generally, the values of surface areas calculated applying different methods increase after the oxidation of the initial carbon A. Remarkable changes in the pore volumes determined by different methods after oxidation of carbon A are not observed. Summing up, the influence of this process on porosity is small since it leads to the blocking of the smallest and/or narrowing of the wider micropore entrances, respectively [87,88,91,92]. These results are similar to those observed previously [87,88,91,92]. On the other hand, it can be noted that the investigated samples (carbon A and B) possess values of apparent BET surface areas (Table 4) close to those observed to typical commercial carbons [11]. The total volumes of mesopores evaluated by the DFT method (0.081 and 0.078 cm^3/g, respectively), as well as their surface areas (5.2 and 9.8 m^2/g, respectively), are very small and similar to those observed for strictly microporous carbonaceous films (where the majority of micropores possess the same diameter ($\sim 0.4 < L <\sim$ 0.6 nm) [30]). On the other hand, the analysis of the differential pore size distributions ($J(L - d_a)_{DFT}$) calculated for both studied samples (i.e., carbons A and B) indicates that the pores are grouped around three main diameters (Fig. 6). In order to simplify the consideration for both carbons two groups of micropores are assumed to be present (first and second are analyzed jointly). The first one approaches diameters equal to 0.7–1.0 nm (i.e., $L <\sim 1.0$ nm) whilst the second one oscillates in the range 1.0–2.0 nm. In Table 4 the parameters of the primary and secondary porous structure (determined from DFT for manual choice regularization parameter λ equal to 1×10^{-5} [53,74,103,104]) are included ($L_{av,DFT,I}$ and $L_{av,DFT,II}$, respectively) and compared with those evaluated from the Nguyen and Do model [49–56]. It is seen that the volume of the primary micropores ($V_{DFT,I}^{micro}$) contributes about 51.2% (carbon A) or 59.2% (carbon B) to the total volume of pores. Moreover, 78.2% (carbon A) and 81.1% (carbon B) (Table 4) of pores smaller and/or equal to 2 nm in the total volume of all pores is observed. Therefore, studied carbons can be regarded as microporous solids with dispersed microporosity (Fig. 6). The results achieved from the high-resolution α_s-plot method (Fig. 7) and the new method of calculating the pore-size distributions proposed by Nguyen and Do (ND theory) confirm this statement (Fig. 6). The shapes of the high-resolution α_s-plots (the FS/CS type, following the classification proposed by Kaneko et al. [105]) observed for both studied samples (Fig. 7) led

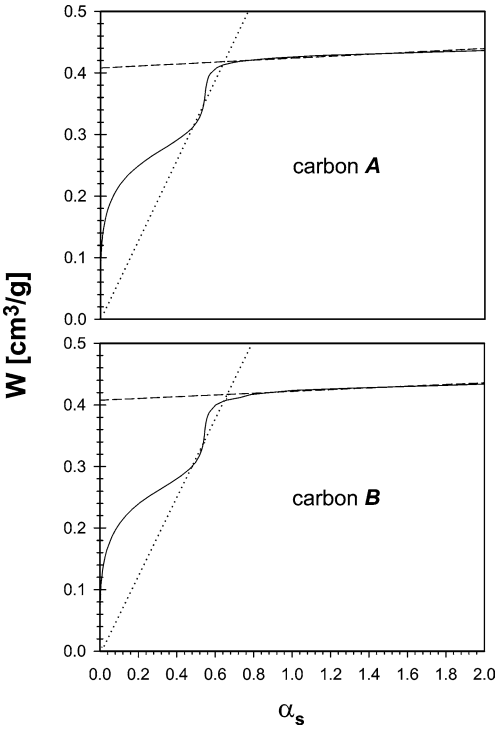

Fig. 7. High-resolution N_2 ($T = 77.5$ K) α_s-plots obtained using graphitized carbon Sterling FT-G as the reference system (the same type of plots, i.e., FS/CS is obtained).

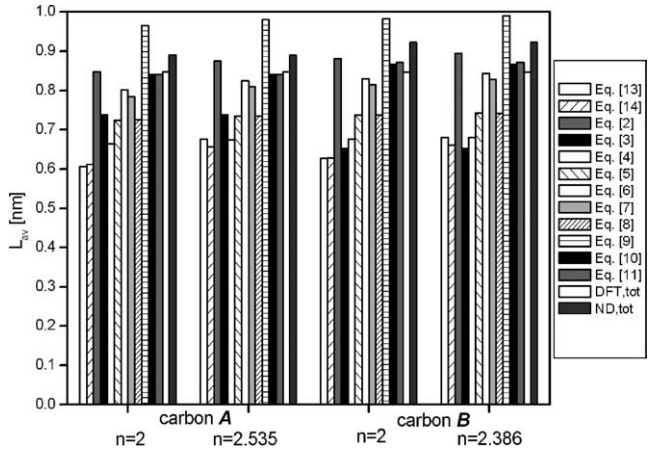

Fig. 8. The comparison of the average pore diameters obtained from Eqs. (2)–(11), (13), (14) and DFT and ND methods ($L_{av,DFT,tot}$ and/or $L_{av,ND,tot}$, Table 4). The full range of micropores was considered due to the fact that DA and/or DR equation was fitted to the range of adsorption which takes place in the pores where micropore filling and a cooperative swings mechanism occur.

to the suggestion that they posses the micropores leading to both filling and co-operative swings on α_s-plots. It can be noticed that the linear region is short and this indicates the presence of relatively narrow pores [102]. Summing up, DFT and ND methods suggest a polymodal structure of pores and indicate that the chemical treatment does not significantly influence the porosity. Furthermore, one can notice that the method proposed by Nguyen and Do slightly shifts the dimension of pores to larger diameters in comparison with the DFT results (Fig. 6 and Table 4). Contrary to the methods mentioned above, HK suggests an exponentially decreasing form of the MPSD curves (see Fig. 6). It can be noticed that HK method approximate DFT and ND results reasonably well. Similar situation was observed for studied recently strictly microporous homogeneous carbon films [30]. The HK theory leads smaller (carbon A) and larger (carbon B) pore diameters in comparison with DFT and HK models.

The comparison of calculated average micropore diameters (nitrogen adsorption data are only analyzed) is presented in Table 4 and in Fig. 8. The optimized values of the parameter n of the Dubinin–Astakhov (DA) isotherm equation (Table 5) are close to those assumed in the Dubinin–Radushkevich one ($n = 2$). Therefore, the influence of this parameter on the results obtained based on Eqs. (13) and (14) is insignificant. For all the studied samples, Eq. (9) and the ND method lead to the highest values of the average micropore width, while Eqs. (13) and (14) in most cases lead to the lowest ones. Results similar to the DFT are the most frequently obtained for Eqs. (6), (10), and (11). It can be seen that a good correlation between calculated results based on relations proposed by us (i.e., Eqs. (13) and (14)) and the results obtained from DFT and/or ND methods can not be obtained (although, PSDs are comparable). In contrary to activated carbons analyzed in the current paper, the similarity was obtained previously for the more strictly microporous adsorbents—carbonaceous films [30]. This is the consequence of the more homogeneous structure of the micropores [30]. For carbon A and B micropores are significantly dispersed (Fig. 6). Therefore, the values of the average widths calculated based on monomodal PSDs as well as pore-size distributions obtained from the HK method (Fig. 8) are shifted to smaller values in comparison with DFT and/or ND values.

To discuss the possibility of the existence of similarity between the Horvath–Kawazoe and ND (or DFT) methods in the next figures (Figs. 9 and 10) we present the results of the analysis of modeled DA isotherms, described by the above-mentioned theories [35]. In Fig. 9 the influence of n (the parameter of the DA equation) on the $J(L - d_a)$ function is shown for $E_0 = 25$ kJ/mol. It can be noticed that the increase in n leads to an increase in maximum value of this function (and narrowing of the distribution is observed simultaneously) for the HK model (Fig. 9—lines). The evaluated values of $(L - d_a)$ related to the maximum of MSD are similar. Moreover, the result of the numerical differentiation provides a decrease in L_{av} value with the increase in n at constant E_0. On the other hand, PSD curves calculated form the ND model (Fig. 9, bars) show that for high n an almost homogeneous pore system is observed (the dispersion of pore diameters is around the diameter of one nitrogen molecule). The decrease in the n value leads to a decrease in the intensity of the peak and the second peak appears in the range of pores with diameters around 1.5 nm. Thus, the de-

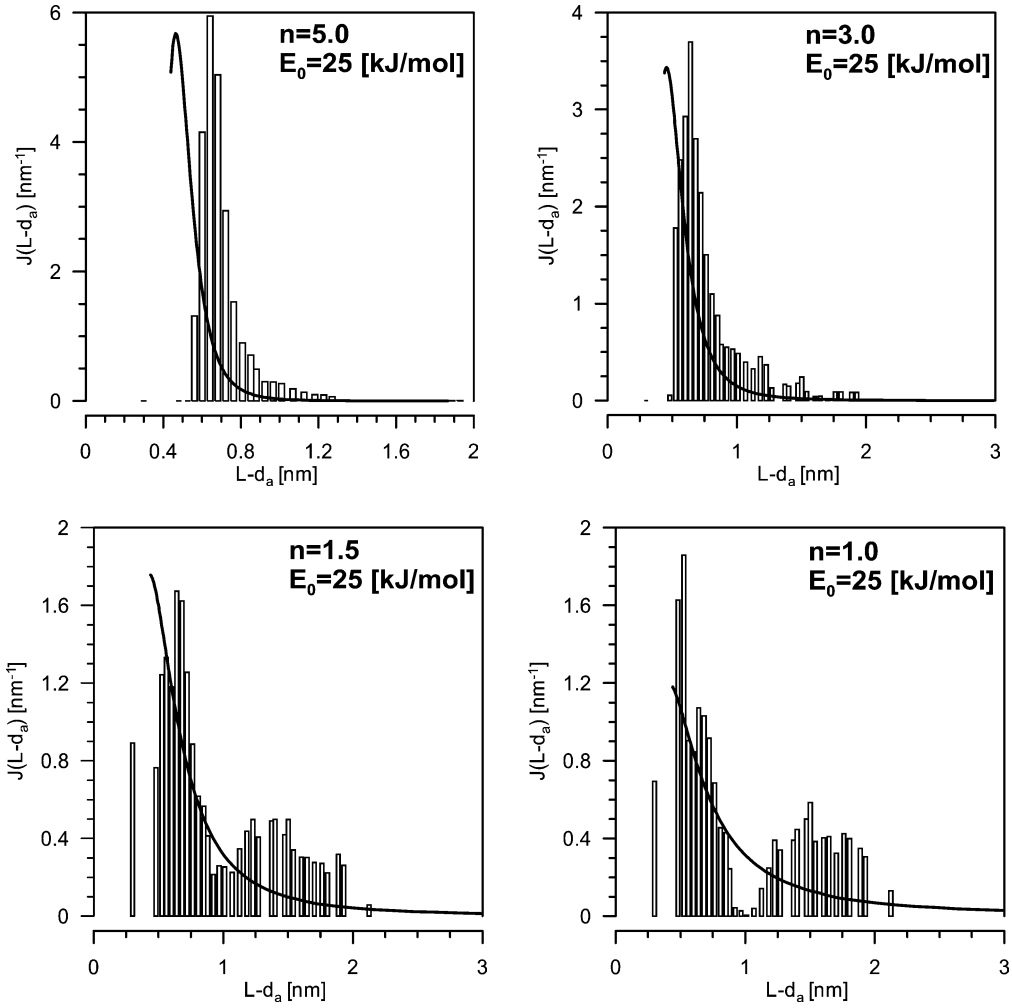

Fig. 9. The influence of parameter n on the $J(L-d_a)$ calculated for N_2 ($E_0 = 25$ kJ/mol); bars—the Nguyen–Do method; lines—the Horvath–Kawazoe method.

crease in n value (at constant E_0) leads to the conversion of the PSD from monomodal to bimodal. Moreover, a negligibly small amount of mesopores are present for $n = 1$. The detailed analysis of the Nguyen and Do models suggested that for the first group of isotherms (constant energy, different n values) a decrease in n leads to the conversion of α_s–FS plots into FS/CS [35], suggesting the transformation of the mechanism of adsorption in micropores from primary micropore filling into simultaneous primary and secondary micropore filling.

In the next figure (Fig. 10) the influence of the parameter E_0 on the $J(L-d_a)$ calculated for N_2 ($n = 3.0$) is shown. In this case, the analysis of the results obtained from the HK theory shows that the increase in the characteristic energy of adsorption leads to decrease in maximum value of $J(L-d_a)$ and increase the related to them values of $(L-d_a)_{p,\max}$ (Fig. 10—lines). It can be noticed that for the largest energy value an almost homogeneous PSD is obtained from the ND method (Fig. 10—bars). In the range of E_0 20–25 kJ/mol bimodal PSD is observed, as a result of the decrease in the intensity of the peak around 0.7 nm, and the increase in the intensity of the peak related to the adsorption in wider pores (ca. 1.2 nm). For the smallest analyzed value of energy the first peak vanishes completely and only the second is visible. The same changes as those observed on PSD curves occur also on α_s-plots. For the largest values of energy (40 and 32 kJ/mol) the obtained α_s-plots belong to the FS group, and the CS swing is almost absent. The decrease in energy value leads, however, to the creation of two swings; thus, for E_0 in the range 20–25 kJ/mol, FS/CS-type α_s-plots are observed. For the smallest energies, the α_s-plots become the typical CS type [35].

It can be seen that the similarity between the both methods occurs only for isotherms describing primary micropore filling process (i.e., FS type of swing in the high-resolution α_s-plot is observed). Therefore, since the relations (Eqs. (13) and (14)) are based on the HK adsorption potential, they lead to results similar to those obtained from ND (DFT, GCMC) methods, only for carbons possessing very narrow micropores. The results presented in this section lead to the statement that for microporous carbons where a primary micropore filling process predominates (especially, strictly

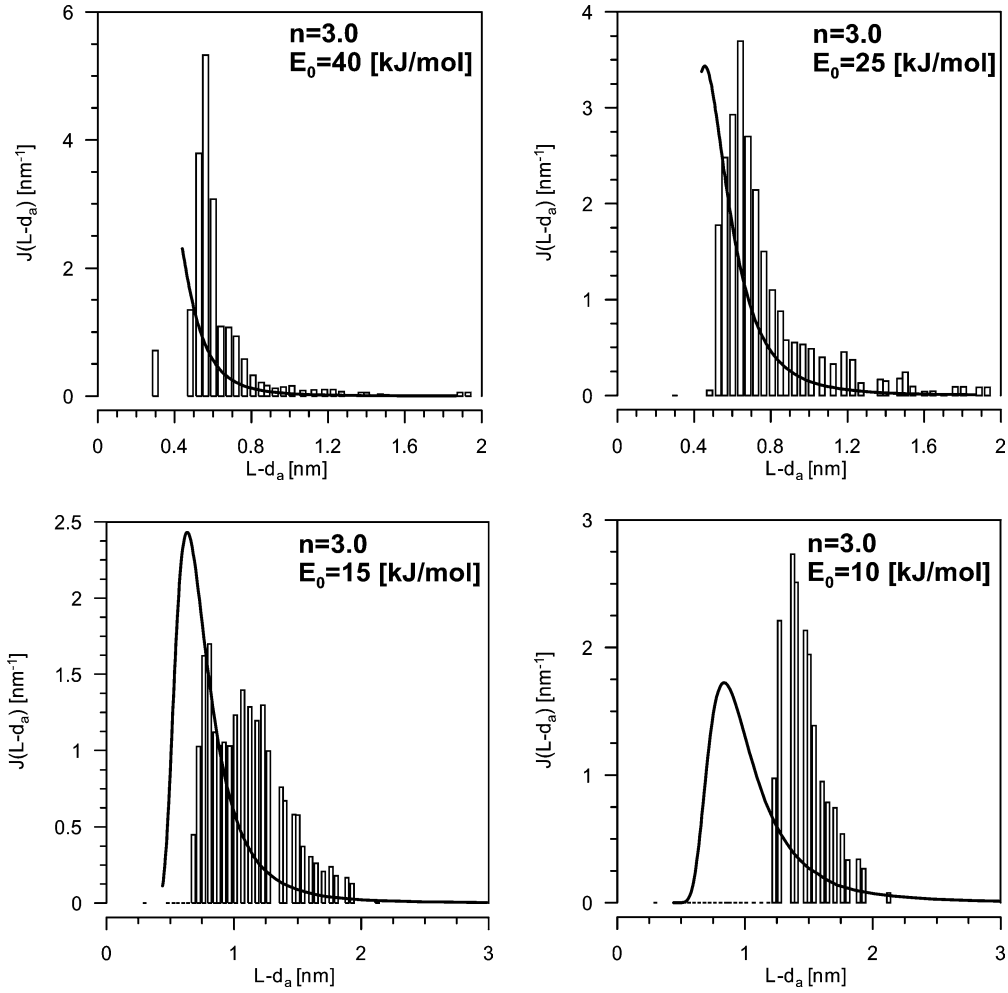

Fig. 10. The influence of parameter E_0 on the $J(L-d_a)$ calculated for N_2 ($n = 3.0$); bars—the Nguyen–Do method; lines—the Horvath–Kawazoe method.

microporous), similarity exists between DFT and HK methods [7,30,31,59,74]. Therefore, the HK model is, as a matter of fact, the simplest method of microporosity characterization leading (in some cases) to results similar to those obtained from DFT or ND methods. The differences between those methods vanish if the existence of wider micropores can be neglected. Summing up, the HK method is effective for highly microporous carbons possessing the pores having similar width.

3.3.2. Pore size distributions—the influence of adsorbates

The comparison of the experimental adsorption data of Ar, N_2, CCl_4, and C_6H_6 on activated carbon: A (open symbols) and B (closed symbols) is given in Fig. 2. All adsorption isotherms belong to I type of IUPAC classification [93]. Moreover, the small influence of the type of adsorbent on the plots is observed. The comparison of adsorption data shown in Fig. 2 (the experimental data) and Figs. 5a and 5c (theoretical ones) suggests similar sequences of the isotherms, but for C_6H_6 the difference is more significant. It is necessary to remember that the theoretical DA adsorption isotherms (Eq. (1)) are plotted for all analyzed adsorbates based on the same values of the characteristic energy ($E_0 = 25$ kJ/mol) and parameter n (=3.0). The optimized parameters are obtained from the fitting of the theoretical equations (DR and/or DA) to experimental data (up to the relative pressure ca. 0.1 as was mentioned above). They are collected in Table 6. The analysis of W_0, E_0, and n shows that the difference between those parameters for the two carbons are irrelevant. The highest discrepancy between the results of the calculation based on DA and DR is achieved for CCl_4 (the largest molecule—Table 1). For all investigated systems the evaluated values of the determination coefficient are satisfactory (DC close to 0.98 and higher) and for all the cases $DC_{DA} > DC_{DR}$.

As described above it is possible, based on the HK theory, to achieve the same PSDs for different adsorbates. However, the comparison of the hypothetical values of both parameters of the DA equation with the calculated from experimental data suggests that the pore size distribution curves should be slightly different. The experimental data confirm this presumption. The comparison of the differential micropore-size distributions calculated for carbon A and B using the DFT (N_2), HK (Ar, N_2, CCl_4, and C_6H_6) and ND (Ar, N_2, CCl_4,

Table 6
The comparison of the average pore diameters obtained from Eqs. (13) and (14) for all investigated adsorbates

Carbon	L_{av} (nm)			
	DA—Eq. (1)		DR—Eq. (1), $n = 2$	
	Eq. (14)	Eq. (13)	Eq. (14)	Eq. (13)
		Ar		
A	0.882	0.868	0.936	1.072
B	0.902	0.915	0.940	1.079
		N_2		
A	0.612	0.606	0.657	0.676
B	0.628	0.627	0.661	0.681
		CCl_4		
A	0.898	0.933	0.911	0.996
B	0.991	1.099	0.967	1.094
		C_6H_6		
A	0.699	0.922	0.895	0.991
B	0.714	0.820	0.884	0.972

and C_6H_6) methods, are presented in Fig. 11. It can be noted that the calculated HK pore-size distribution curves for some adsorbates are very similar (especially for N_2, Ar, and C_6H_6), and they cover practically the same ranges of pore diameters; but sometimes they significantly differ (CCl_4). The location and the shape of the MSDs strictly depend on an adsorbate. For example, the MSD estimated on the basis of the N_2 adsorption isotherm is similar to an exponential and suggests that the main portion of pores are located in effective micropores with width greater than 1 nm for both carbons. The shapes and location of distributions obtained from Ar and C_6H_6 adsorption isotherms are very similar. Here the main portion of micropores is shifted to larger pores (0.6–0.8 nm) for the considered adsorbents. The MSD obtained from CCl_4 data clearly shows that the main portion of micropores is located between 0.9–1.2 nm. The pore size distribution curves calculated from the ND model (and presented in Fig. 11) are different from those obtained from the HK theory. The location and the shape of the MSDs strictly depend on an adsorbate. It can be noticed that the calculated ND pore-size distribution curves for some adsorbates cover practically the same range of pore diameters; but sometimes they significantly differ (CCl_4 and N_2). On the other hand, the shapes and location of the distributions obtained from Ar and C_6H_6 adsorption isotherms are very similar. The pore-size distributions form ND method are shifted to larger pore diameters in comparison with the HK model and this is caused by the differences in the pore filling pressure vs pore diameter curves as shown in Fig. 3.

On the other hand, the values of E_0 and n (collected in Table 5) are used for the calculation of the average pore diameters based on Eqs. (13) and (14) for all analyzed adsorbates. Thus, the present studies are limited only to the theoretical relationships proposed previously [28–34]. The final results are compared in Table 6. The main aim of current paper is the analysis of the influence of the diameter of the adsorbates (d_A) and the temperature (T) on the average diameter of micropores (L_{av}) and PSDs. Assuming a lack of swelling (the geometric invariance of the adsorbent during the adsorption process), one can take into consideration the correlation between the accessibility of the adsorbed molecule (and the diameter of this molecule) to the microporous structure of an adsorbent and the pore widths. The analysis of data collected in Table 6 establishes the following sequence of adsorbates with respect to the increase of the average widths of micropores: $N_2 < C_6H_6 < Ar < CCl_4$. This sequence is the same as obtained for the above-mentioned MSDs. Nitrogen molecules are the smallest ($d_A = 0.300$ nm; Table 1). Therefore they can penetrate the finest micropores—lower average pore widths are obtained (Eqs. (13) and (14)). Ar diameter ($d_A = 0.336$ nm; Table 1) is larger than N_2 and that is why for this adsorbate larger average pore widths are evaluated. A similar situation is observed for CCl_4 ($d_A = 0.465$ nm). For this adsorbate the differential pore size distributions should lie between Ar and C_6H_6 (if the influence of the adsorbate diameters is analyzed only). But for experimental data (Fig. 11) a different situation is observed due to an exception to the rule for C_6H_6 ($d_A = 0.459$) nm. Apparently, the mutual position of $J(L - d_a)$ decides not only d_A but also the temperature and the parameters characterizing an adsorbate (Fig. 5a). It is necessary at this moment to remember that Ar, CCl_4, or C_6H_6 experimental adsorption isotherms are measured in various temperatures.

3.3.3. Calorimetric data

As mentioned above, the thermodynamic verification of the most popular methods of porosity determination of the carbonaceous adsorbents (DFT, HK, and others) is rarely met in the literature (mainly the Polanyi–Dubinin theory of adsorption was successfully verified [106]). It is well known that the measurement of the enthalpy of adsorption can lead to very interesting information about the mechanism of adsorption process as well as about the energetic and structural heterogeneity of adsorbents [32,87,88,91,92]. Moreover, one of the methods of a theoretical model verification is to check the applicability of the both adsorption isotherm and related enthalpy equations for the description of experimental adsorption and heat of adsorption data (sometimes other thermodynamic functions are also analyzed). It should be pointed out that the HK model was derived based on thermodynamic assumptions (the details can be found elsewhere [25,38,42,43,68–72]). One of the most important postulation of this model is the assumption that the adsorbed phase is considered to have the similar properties as liquid. Therefore, the above mentioned condition should be fulfilled by [42,43]

$$|T\Delta S^{\mathrm{ads}}| \ll |q^{\mathrm{diff}}|, \tag{16}$$

where T is the absolute temperature, ΔS^{ads} is the entropy of adsorption and q^{diff} is the differential heat of adsorption. In other words, Horvath and Kawazoe suggested, using experimental data, that the entropy term is negligible in the

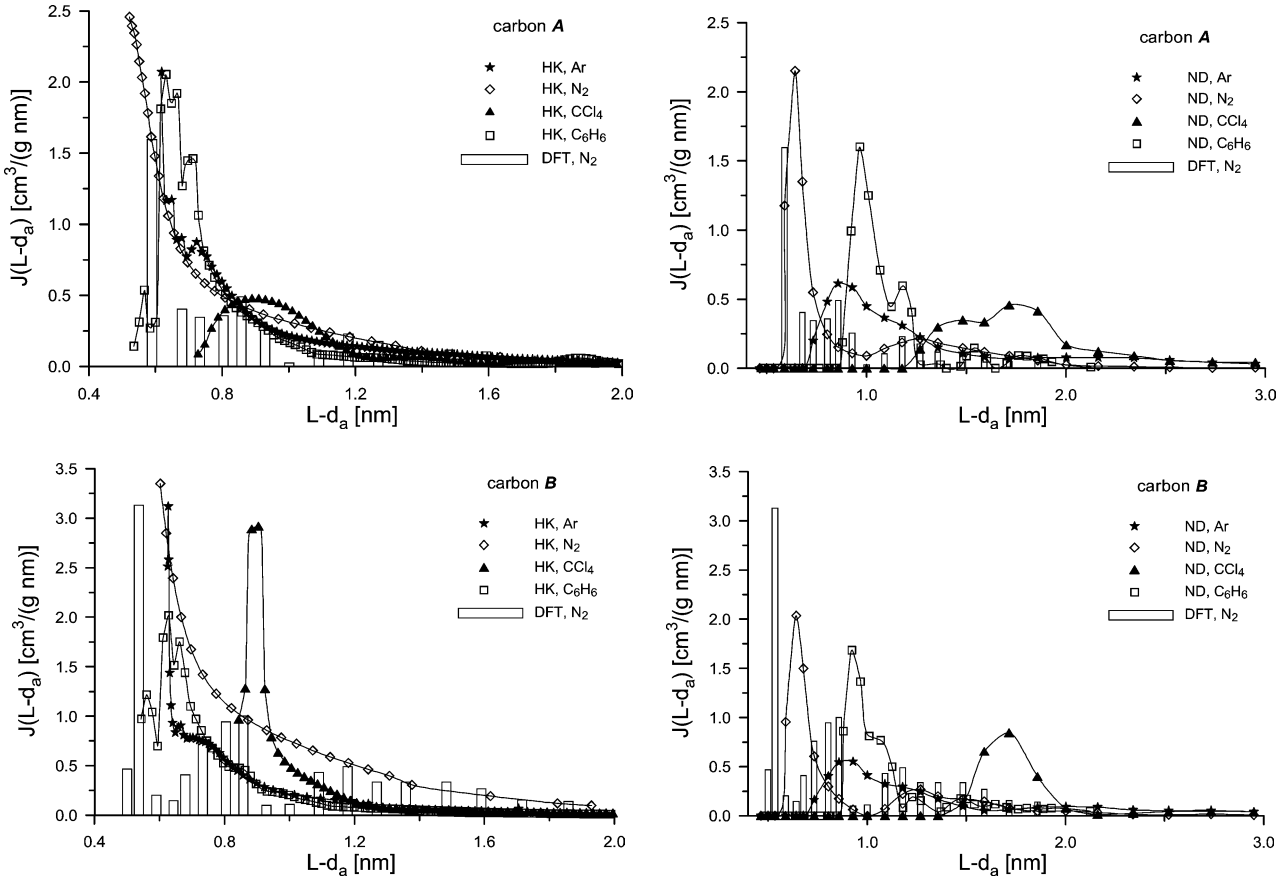

Fig. 11. The comparison of the differential micropore-size distributions calculated using DFT (N_2) and HK or ND (Ar, N_2, CCl_4, and C_6H_6) methods. The pore-size distributions calculated based on the DFT model are treated as the reference.

circumstances mentioned above. They used the N_2 isotherm adsorption data (77.5 K) measured on strictly microporous molecular sieve carbon HGM 638, and calculated q^{diff} based on the simplified relation [42,43]

$$q^{\text{diff}} = \Delta G^{\text{ads}} - \Delta H^{\text{vap}}, \tag{17}$$

where $\Delta G^{\text{ads}} = -A_{\text{pot}}$ and ΔH^{vap} is the enthalpy of vaporization (equal with minus sign to the enthalpy of condensation, L). Horvath and Kawazoe noticed the similarity of the data calculated based on Eq. (17) with the "experimental" isosteric heat of adsorption obtained from isotherms measured at different temperatures.

It should be pointed out that the HK model has been verified only for one set of experimental data and we do not find other cases in the literature. Therefore, we decided to perform the thermodynamic verification for both samples studied in this paper. The calorimetrically measured enthalpies of adsorption of C_6H_6 and CCl_4 are shown in Figs. 12 and 13. Moreover, these data will be applied to calculate, using the method published by Everett and Powl [44], the enhancement of potential energy in micropores in comparison to the energy of adsorption on a "flat" surface.

Knowing adsorption isotherms and the differential molar heats of adsorption, the differential molar entropies of adsorbed molecules (S^{diff}) can be calculated by [92]

$$S^{\text{diff}} = S_g - (q^{\text{diff}}/T) - R\ln(p/p_0) + R, \tag{18}$$

where S_g is the molar entropy of the gas at the temperature T (for C_6H_6 at 313.15 K it is equal to 273.1 J/(mol K) [107] and for CCl_4 at 308 K it is equal to 315.50 J/(mol K) [107]), and p_0 is the standard state pressure. It is well known that different standard states can be chosen, and in our case, the gas at the standard pressure of $p_0 = 101325$ Pa was applied.

We also calculated the enthalpy and entropy of adsorption basing on the potential theory and applying the procedure described previously [106]. Assuming the fulfillment of the main condition of the potential theory (first of all the temperature invariance condition $(\partial A_{\text{pot}}/\partial T)_{\Theta} = 0$), we obtain

$$\Delta H^{\text{ads}} = -A_{\text{pot}} - \frac{\alpha T \Theta}{F(A_{\text{pot}})}, \tag{19}$$

$$\Delta S^{\text{ads}} = -\frac{\alpha \Theta}{F(A_{\text{pot}})}, \tag{20}$$

where $F(A_{\text{pot}}) = -d\Theta/dA_{\text{pot}}$ is the differential adsorption potential distribution. Therefore, for the Dubinin–Astakhov equation (Eq. (1)) the differential heat of adsorption and the differential molar entropies of adsorbed molecules are

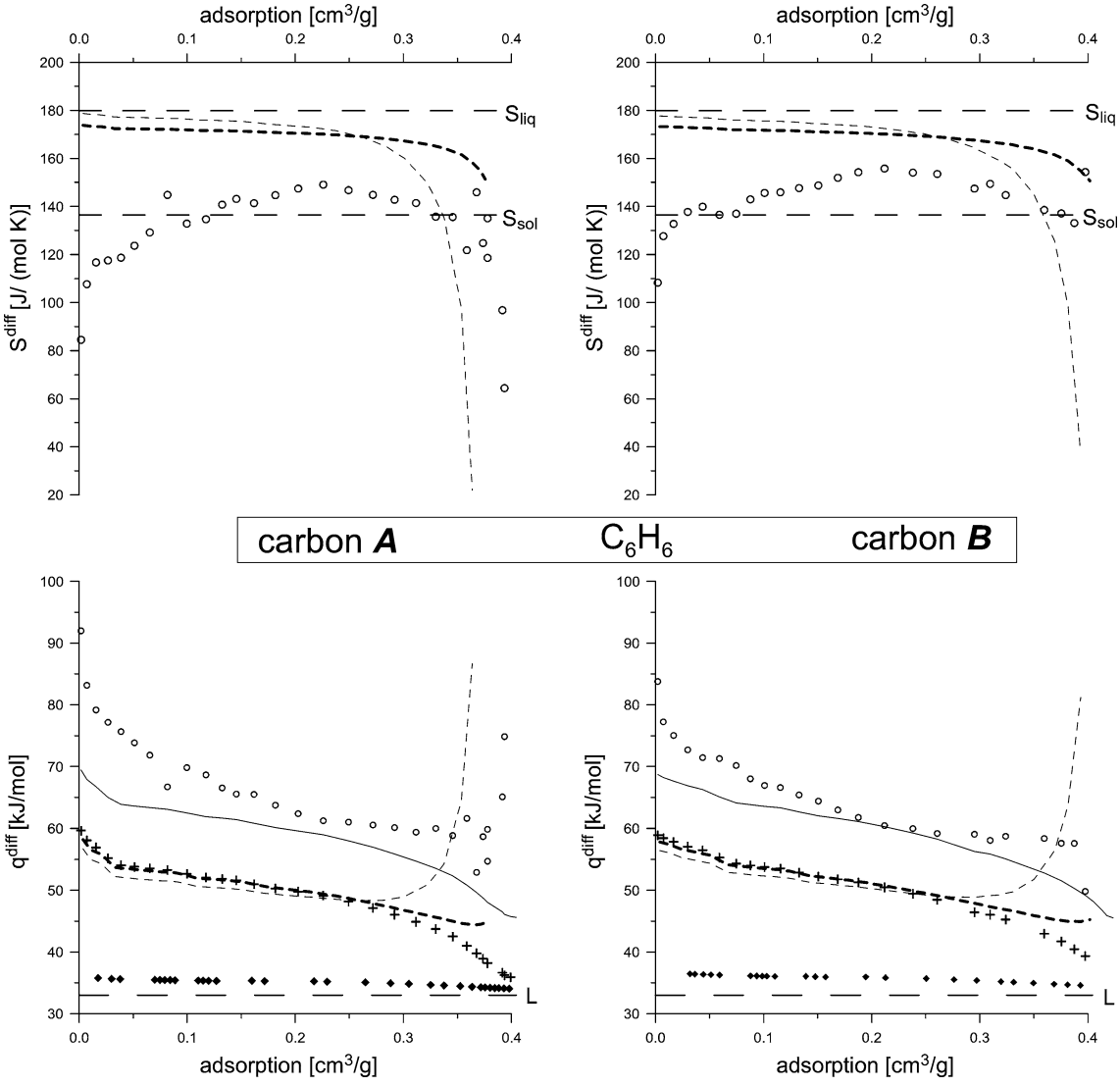

Fig. 12. The experimental data (circles) measured for C_6H_6 on carbon A and B ($T = 313$ K). Entropy: the differential molar entropy of adsorbed C_6H_6 calculated based on Eq. (18) (circles); Eq. (22) (thin or bold dashed lines (for the DA or DR equations, respectively)); horizontal dashed lines—the values of the entropy of liquid ($S_{liq} = 179.89$ J/(mol K)) and solid ($S_{sol} = 136.50$ J/(mol K)) benzene. Enthalpy: the differential molar enthalpy measured calorimetrically (circles) and calculated based on: Eq. (17) (crosses); Eq. (23) (solid line); Eq. (21) (thin or bold short dashed lines (for the DA or DR equations, respectively), $\alpha = 1.16 \times 10^{-3}$ K^{-1} [97]); the model proposed by Nguyen and Do (closed symbols); horizontal dashed line—the value of the enthalpy of condensation ($L = 33.042$ kJ/mol [97]).

given by

$$q^{\text{diff}} = A_{\text{pot}} + \frac{\alpha T \Theta}{F(A_{\text{pot}})} + L - RT$$
$$= A_{\text{pot}} + \frac{\alpha T \beta E_0}{n} \left(\frac{A_{\text{pot}}}{\beta E_0} \right)^{1-n} + L - RT \qquad (21)$$

and

$$S^{\text{diff}} = S_{\text{liq}} + \Delta S^{\text{ads}} = S_{\text{liq}} - \frac{\alpha \beta E_0}{n} \left(\frac{A_{\text{pot}}}{\beta E_0} \right)^{1-n}, \qquad (22)$$

where α is the coefficient of the adsorbate thermal expansion (the meanings of other parameters are presented in the previous sections and in Appendix A).

On the other hand, the calculations of the enthalpy of adsorption from ND method were performed adopting the procedure described by Nguyen and Do [108]. The authors assumed that the decrease in the potential energy of adsorbate molecules is the principal source of heat released during the adsorption process. For micropores, where the solid–fluid interaction is much more significant than the fluid–fluid interaction, the potential change, which is calculated using the Lennard–Jones energy equation, can be taken as the first approximation to the heat of adsorption. The heat released from individual micropores at any stage of adsorption can thus be evaluated. Based on the procedure proposed by Nguyen and Do the total heat at any overall loading can be estimated by summing up the heats from individual pores—this is the cumulative heat produced when the fixed amount is loaded into a clean sample. Next, the differential heat of adsorption is calculated; i.e., it is the incremental heat pro-

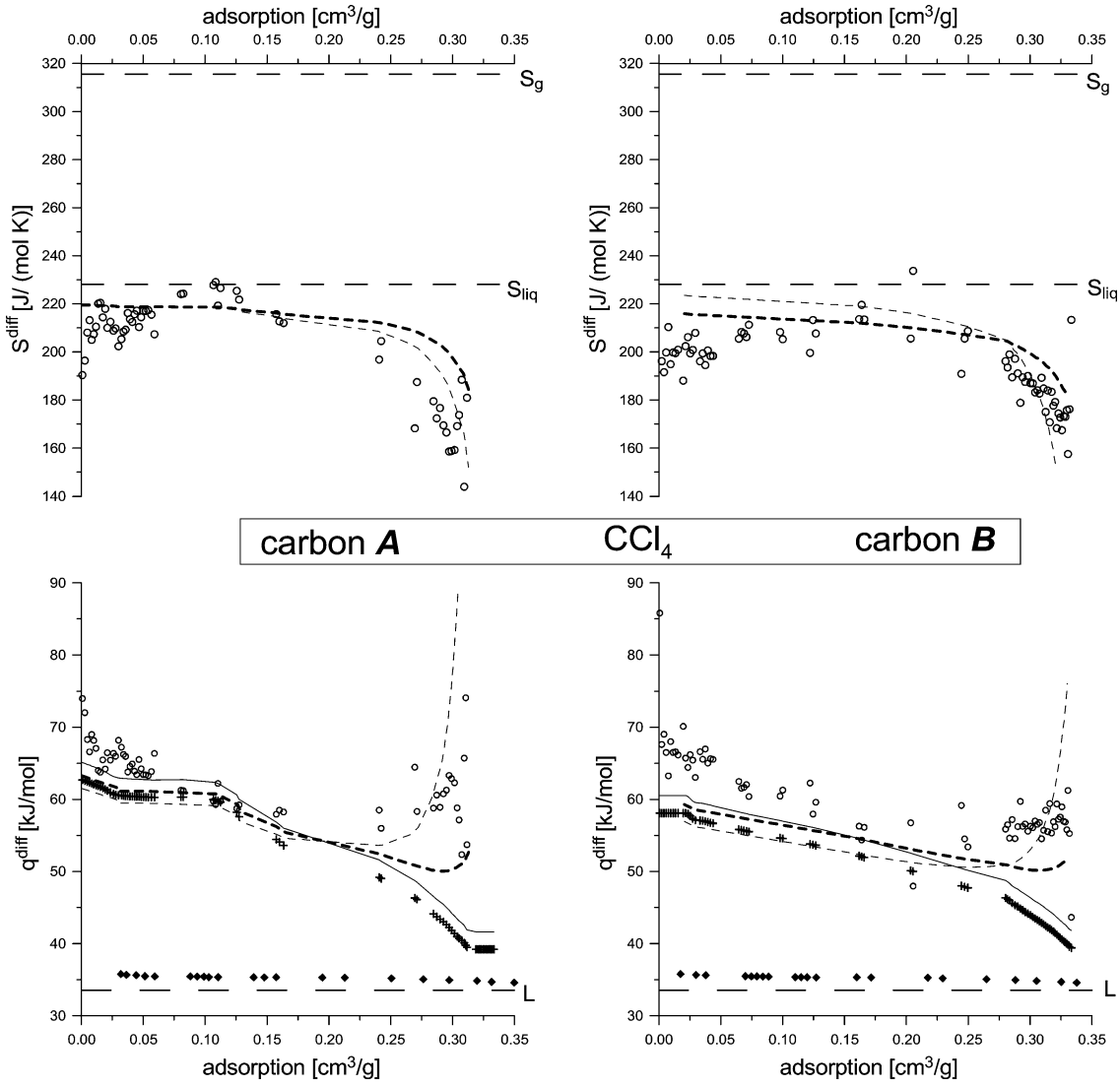

Fig. 13. The experimental data (circles) measured for CCl_4 on carbons A and B ($T = 308$ K). Entropy: the differential molar entropy of adsorbed CCl_4 calculated based on Eq. (18) (circles); Eq. (22) (thin or bold dashed lines (for the DA or DR equations, respectively)); horizontal dashed lines—the values of the entropy of liquid ($S_g = 315.5$ J/(mol K)) and liquid ($S_{liq} = 228.1$ J/(mol K)) carbon tetrachloride on carbon. Enthalpy: the differential molar enthalpy measured calorimetrically (circles) and calculated based on Eq. (17) (crosses); Eq. (23) (solid line); Eq. (21) (thin or bold short dashed lines (for the DA or DR equations, respectively), $\alpha = 1.22 \times 10^{-3}$ K^{-1} [97]); the model proposed by Nguyen and Do (closed symbols); horizontal dashed line—the value of the enthalpy of condensation ($L = 33.545$ kJ/mol [97]).

duced per mole when the loading is incrementally increased from lower value of adsorption to upper one. The details of calculations are given in [108].

The final results of the calculation of the thermodynamic functions (i.e., q^{diff} and/or S^{diff}) are shown in Figs. 12 and 13. In order to compare the experimental and theoretical data of enthalpy of adsorption the state of C_6H_6 and CCl_4 molecules in micropores should be investigated based on the differential molar entropies of adsorbed molecules (S^{diff}). It can be seen that the values of the differential entropy of adsorbed benzene falls close to the value characteristic of a solid ($S_{\text{sol}} = 136.50$ J/(mol K) [109], especially for carbon A (Fig. 12). Furthermore, the entropy of the CCl_4 on the same carbons is lower than the entropy of liquid ($S_{\text{liq}} = 228.10$ J/(mol K) [109]). However, it is interesting to compare the plots of the entropy of adsorption presented in Figs. 12 and 13 with those obtained previously [30] for the carbonaceous films (the benzene data are only analyzed) possessing more homogeneous pore structure than carbons A and B. As it can be seen from our previous study [30], 88% of micropores of films possess the same diameter (0.536 nm, and the volume 0.178 cm^3/g, determined from DFT for N_2 adsorption) and that is the reason why the plot of the integral molar entropy of adsorbed C_6H_6 is almost constant (Fig. 7 in [30]). As it can be noticed, for the higher values of adsorption the increase in differential entropy occurs, and this is caused by the commence of adsorption in the secondary structure of pores where differential entropy approaches to the value characteristic of a liquid. Comparison of the differential entropy of benzene adsorption on

both type of adsorbents (i.e., polyfurfuryl carbons, Figs. 12 and 13 (in the current study), and carbonaceous film, Fig. 7 in [30]) shows that the increase of S^{diff} is observed (bringing closer to S_{liq}) for the adsorbent possessing wider pores. Summing up, small differences in the entropy of adsorbate molecules and the quasi-solid state are still observed (it can be noticed that one of the most important postulation of the HK model, i.e., the adsorbed phase is considered to have the properties similar to those of the liquid phase, is not correct in this case). As was shown recently [30,91,92], for the cases where the adsorbed molecules approach to the state of quasi-solid, the equations of the potential theory of adsorption (Eqs. (21) and (22)) do not describe the calorimetric data (usually too low enthalpy values are observed comparing to the experimental ones). It is obvious that a liquid state was taken as the reference during the performance of the calculation from the potential theory. Therefore, these differences may be caused by the incorrect assumption of the liquid state of an adsorbate.

Knowing that, for a perfect gas and for the standard state of 101325 Pa, the entropy of benzene is equal to 273.08 J/(mol K) (and the translational entropy contributes 164.10 J/(mol K) to this value), it can be clearly seen that almost all three translational degrees of freedom are lost by adsorbed molecules. Similar effect was observed for adsorption of benzene by a microporous silica [110]. We showed recently [92], for the series of adsorbates, that the entropy, as well as the other thermodynamic properties of molecules confined in pores, can approach values characteristic of a quasi-solid. Watanabe and co-workers [111] stated, based on DSC results, that the "liquid" state of C_6H_6 confined in micropores should be partially ordered, while the "solid" state should be disordered due to serious geometrical restriction of the formation of a well-crystallized solid structure. Babaev and co-workers [109], who studied the enthalpy of C_6H_6 adsorption on an activated carbon AC, reported similar effect. They noticed a substantial decrease in the entropy of adsorbed benzene from the value characteristic of the enthalpy of a liquid to a value lower than the enthalpy of a solid (the average value of entropy was 155 J/(mol K) and, thus, was located between the value characteristic of a liquid and the entropy of a solid, respectively). In the current study, the values of entropy slightly lower than those reported by Babaev and co-workers are observed, and this is caused by the differences in the porosity of the studied samples. The carbon AC studied by those authors possessed also mesopores (5% of total volume of pores; their radius calculated on the basis of hysteresis using the Kelvin equation was close to 2 nm; this method cannot be treated as the reliable one). Moreover, micropores wider than those of the sample studied by us previously [30], as well as a wider dispersion, were observed for carbon A and B (current studies) and AC [109]. Babaev and co-workers [109] noticed that "for the wide distribution of micropores it is impossible to find the fraction of micropores with diameters close to the diameter of C_6H_6 molecule, in which adsorbed molecules would lose all the translation and rotational degrees of freedom."

The similar results have been observed for other adsorbates than benzene. The combination of differential scanning calorimetry and incoherent elastic neutron scattering has been used by Castro and co-workers [112] to demonstrate the formation of solid layers adsorbed onto graphite from pure alkanes and binary alkane mixtures. Then, they suggested that as fluid molecules are strongly bound on the solid surface, phase transition of the adsorbed layer is often different from that of bulk fluid. Miyahara and Gubbins [113] have suggested that when interaction potential energy of a molecule with the pore wall is grater than that with the pore wall consisting of adsorbate molecules, the melting temperature should be elevated with decreasing pore width and the melting process disappears in micropores. Kaneko and co-workers [114–116] showed, with the aid of in situ X-ray diffraction, that for some adsorbates (for example, CCl_4 molecules) confined in graphitic micropores form a molecular assembly having a more long-range order than the bulk liquid. Summing up, if the graphite micropores were considered, an anomaly of phase transition even for small molecules should be observed. Adsorbate molecules formed a partially ordered structure in the micropore even near room temperature. An unusual elevation of the freezing point of strongly confined fluids have been predicted by theoretical investigations and an experimental evidence for the freezing point elevation using adsorbate molecules confined in the graphite slit nanopores have been observed. This leads to the conclusion that the entropy of C_6H_6 and CCl_4, as well as the other thermodynamic properties of molecules confined in narrow micropores (the analysis of the dispersion of micropores shown in Figs. 6 and 11) can approach the values characteristic of quasi-solid (a partially ordered structure).

The data of the measured heats of adsorption are shown in Figs. 12 and 13. Using the same procedure as previously published by Horvath and Kawazoe [42], the differential heat of C_6H_6 and CCl_4 adsorption is calculated applying the formalism presented above (i.e., Eq. (17)). Final results of the computation are shown in the same figures. It should be emphasized that for the studied carbon samples Eq. (17) describes the experimental C_6H_6 enthalpy data inadequately; i.e., this relation leads to lower heat than measured experimentally, by about 20 kJ/mol. The significantly different situation is observed for CCl_4 data, where the similarity is larger, especially, for lower values of the adsorption. These results suggest that one of the most important postulates of the HK model, i.e., the assumption that the adsorbed phase is considered to have the similar properties as the liquid phase, is not always correct for strictly microporous adsorbents (it is obvious that the same conclusion can be stated for the carbonaceous films [30]). The significant improvement in the description of the benzene experimental data is observed (Figs. 12 and 13), when Eq. (17) is rewritten as

$$q^{\text{diff}} = \Delta G^{\text{ads}} - \Delta H^{\text{vap}} + \Delta H^{\text{cryst}}, \tag{23}$$

where ΔH^{cryst} is the enthalpy of crystallization (equal to 9.84 kJ/mol [97] for C_6H_6 and 2.41 kJ/mol for CCl_4 [97]). This behavior is justified due to the approach that the adsorbed molecules can be treated as a quasi-solid state as described above in detail.

Figs. 12 and 13 show that the enthalpy generated from Dubinin's theory (Eq. (21)) for both carbons and both adsorbates is similar to that generated from the HK model. This is caused by the similar assumptions of both methods, i.e., that in practice the enthalpy of adsorption is reasonably approximated by the change in ΔG^{ads} and the assumption of a liquidlike state of an adsorbate leads to a small contribution of the entropic term (Figs. 12 and 13, thin or bold short dashed lines). As in the case of the HK method for CCl_4 adsorption a better similarity is observed to the enthalpy measured experimentally (the assumption of liquid state is more reliable).

The results of the calculation from the ND method show that this method leads to remarkably lower enthalpy values than measured experimentally. It should be pointed out that this is not the confirmation of the inapplicability of this model (it leads to the same PSD results as the most advanced method—DFT). It is possible that different procedure of the calculation of adsorption enthalpy from this method should be applied. This problem needs further study and the results will be reported.

Using the method published by Everett and Powl [30,44], the enhancement of potential energy in micropores can be evaluated (comparing to the energy of adsorption on a "flat" surface). Thus, calorimetry can be applied as an independent method of the indirect determination of the width of micropores of studied carbons. In order for the Everett and Powl method to be applied the contribution of the functional groups of an adsorbate to the enthalpy of adsorption on microporous carbon must be evaluated. The empirical relationships proposed previously [92] and correlating the adsorption energy with physicochemical parameters of adsorbates are discussed. In Fig. 14 (where the data, published previously (open symbols) and additionally considered in the current paper adsorbate—benzene (diamonds)), it is shown that the initial integral enthalpies (Q^{0A} and/or Q^{0B}), i.e., at so-called "zero coverage" (calculated based on the standard procedures from the differential enthalpy), are correlated with an adsorbate polarizability, α (adsorption on the carbon A) or dielectric constant, ε (adsorption on the carbon B). For the nonspecific adsorbates (without any dipole moment such as methane, carbon dioxide and carbon tetrachloride (Fig. 14a, squares)), the linear relationships (Fig. 14a, dashed line) between enthalpy of adsorption and the adsorbate polarizability is observed (it characterizes the dispersive adsorbate–adsorbent interactions). For the second group, the specific adsorbate–adsorbent interactions contribute to the enthalpy of adsorption at low coverage and, therefore, the relationships between Q^{0A} and α is more complicated (Fig. 14a, solid line). Using the linear relation and knowing the adsorption enthalpy value, and, moreover, assuming the addition of specific and nonspecific interactions, one is able to separate the enthalpy of adsorption into the contribution of the two kinds of energy to this enthalpy. It is interesting to admit that the enthalpy of adsorption at zero coverage on the oxidized carbon (carbon B) can be described by the similar relation, Q^{0B} vs ε (Fig. 14b; solid line) for eight investigated adsorbates. This suggests that for moderately oxidized carbon the specific adsorbate–adsorbent interactions predominate during adsorption in carbon micropores, even at very small coverages. Summing up, it should be stated that the evaluating values of Q^{0A} and/or Q^{0B} excellent verified both theoretical equations proposed previously.

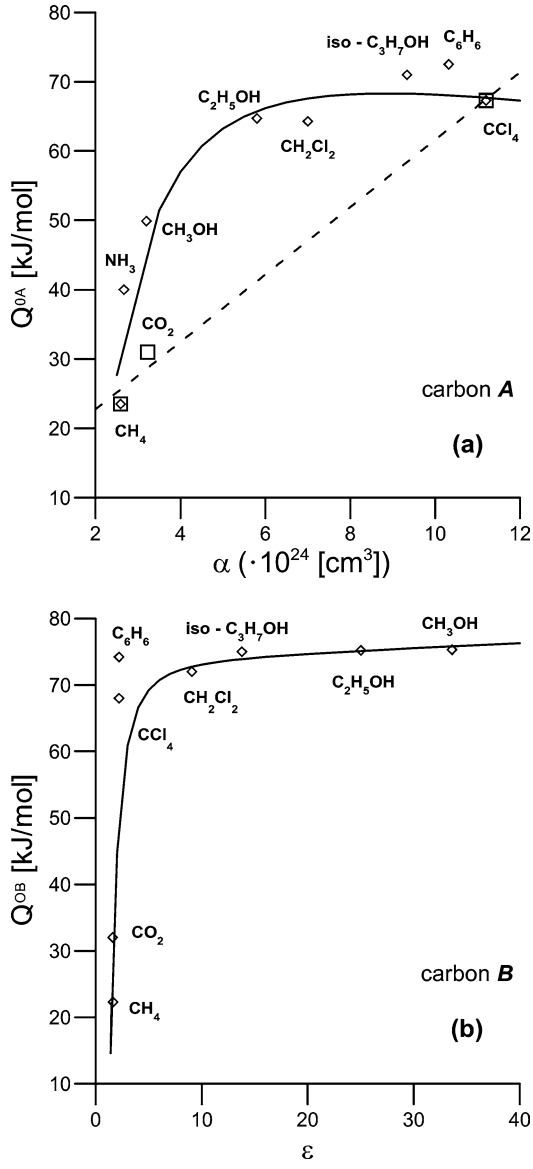

Fig. 14. (a) The dependence of the enthalpy of adsorption on carbon A on adsorbate polarizability (points—experimental data, solid and dashed line—theoretical relationships [88,91,92]). (b) The dependence of the enthalpy of adsorption on carbon B on adsorbate dielectric constant (points—experimental data, solid line—theoretical relationship [88,91,92]).

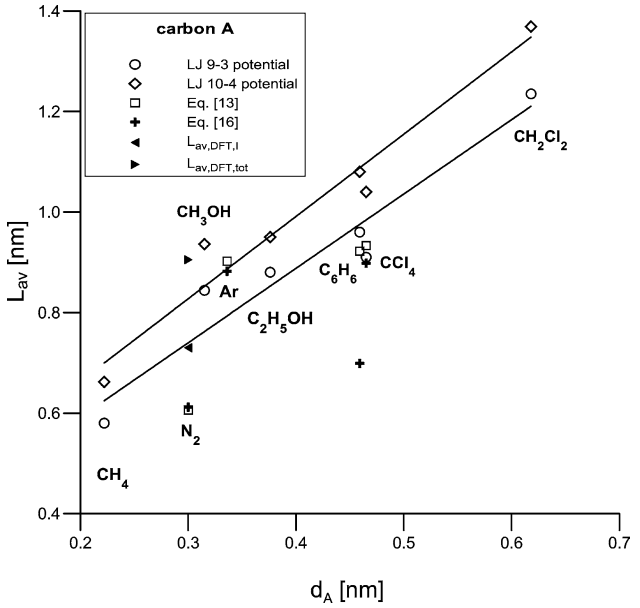

Fig. 15. Carbon A diameters calculated from the enhancement of adsorption potential in micropores (i.e., the Everet and Powl model [44]), the density functional theory and based on Eqs. (13) and (14).

Thus, the integral molar adsorption energies on carbon A can be compared with the enthalpies of adsorption of the same molecules on graphitized carbon black and the enhancement of the adsorption potential in micropores can be calculated. If we assume that adsorption enthalpy at zero coverage is equivalent to the energy of adsorbate–adsorbent interactions, the value of this enhancement is strictly related to the pore diameter. However, as it was shown previously [88,91,92], in the carbon A micropores specific adsorbate–adsorbent interactions enlarge the enthalpy of adsorption of molecules with dipole moments at low coverage. This leads to the conclusion, that the results of the calculation of PSD curves for polar adsorbates (for example, alcohols or water) should be treated with precaution. Fortunately, knowing the value of the potential energy enhancement and using Everett and Powl's theoretical results [44], the carbon A pore diameters can be calculated for benzene and two Lennard–Jones potential models (LJ 10-4 and/or LJ 9-3 [5,44]). Moreover, these results are compared with published previously results for the following adsorbates: CH_4, CH_3OH, C_2H_5OH, CH_2Cl_2, and CCl_4 [88,91,92]. The redrawn results taken from [88,91,92] are shown in Fig. 15 (benzene data are also analyzed) together with pore diameters calculated using different models of porosity determination potentials (LJ 9-3 and LJ 10-4) and based on the low-temperature nitrogen and argon adsorption data (DFT model and Eqs. (13) and (14)). In Fig. 15, the solid lines are plotted applying the proposed general empirical relations between L_{av} and d_A for both potentials [88,91,92]. Thus, the applicability of Eqs. (13) and (14) can be checked using data presented in Table 6 and Fig. 8. It is seen from Fig. 15 that the obtained pore diameters lie close to the lines drawn using empirical equations [88,91,92]. It can be seen that this relation is linear, confirming the occurrence of the molecular-sieve effect and showing again that for application of polar molecule adsorption data to the characterization of porosity, it is necessary to subtract the effect of "specific" interactions occurring even at very low coverages.

4. Conclusions

From the present studies on the adsorption of four adsorbates (N_2, Ar, C_6H_6, and CCl_4) on two microporous adsorbents, the following conclusions can be put forward:

1. All empirical and semiempirical relationships, $L_{av} = f(E_0, n = \text{const})$, generate the decreasing hyperbolic-like function for the typical (and found in the literature) range of the characteristic energy observed for carbonaceous adsorbents. The theoretical relationships, $L_{av} = f(E_0, n)$ give the similar function as empirical ones. The reasons causing differences between pore diameters calculated from various approaches are discussed.
2. It is explained why the HK method gives for some cases the same results as DFT, and is shown that this method is applicable for the carbons where the process of primary micropore filling dominates.
3. The presented results confirm the suggestions of some authors that the PSD is an intrinsic property of the activated carbon (independent of an adsorbate) and the sole source of heterogeneity in spite of different adsorbates having access to different pore size ranges (their difference in molecular size).
4. It is shown that the assumption considering of the adsorbed phase to have the similar properties as liquid is sometimes incorrect for the microporous adsorbents. The significant improvement in the description of the benzene experimental enthalpy data is observed when the enthalpy of crystallization is considered. This behavior is justified due to the approach that the adsorbed molecules can be treated as the state of quasi-solid as was described above in details.
5. Finally, we paid attention to the application of polar molecules adsorption data, for the characterization of porosity of the carbonaceous adsorbents. In our opinion for this type of adsorbate it is necessary to subtract the effect of "specific" interactions occurring even at very low coverages (i.e., the energy of adsorbate–adsorbent interactions can be calculated and next, the energy of specific interactions can be evaluated from the enthalpy of adsorption).

Consequently, the relationship between the phase behavior and pore width of micropores (i.e., micropore-size distribution) of the microporous and mesoporous carbons characterized by the different pore structure needs further studies and the results will be reported in the future.

Appendix A. Nomenclature

ASA	Adsorption stochastic algorithm
A_{HK}	Constant of Eq. (12)
A_{pot}	The free energy of adsorption in Dubinin–Astakhov isotherm equation—Eq. (1) ($\equiv -\Delta G^{ads}$)
$a_{1(all)}$	The parameter of Eq. (13)—shown in Table 2
$a_{1(mic)}$	The parameter of Eq. (14)—shown in Table 3
$a_{2(all)}$	The parameter of Eq. (13)—shown in Table 2
$a_{2(mic)}$	The parameter of Eq. (14)—shown in Table 3
$a_{3(mic)}$	The parameter of Eq. (14)—shown in Table 3
B_{HK}	Constant of Eq. (12)
$b_{1(all)}$	The parameter of Eq. (13)—shown in Table 2
$b_{1(mic)}$	The parameter of Eq. (14)—shown in Table 3
$b_{2(all)}$	The parameter of Eq. (13)—shown in Table 2
$b_{2(mic)}$	The parameter of Eq. (14)—shown in Table 3
$b_{3(mic)}$	The parameter of Eq. (14)—shown in Table 3
C_{BET}	BET constant on flat surface
C_{HK}	Constant of Eq. (12)
$c_{1(all)}$	The parameter of Eq. (13)—shown in Table 2
$c_{2(all)}$	The parameter of Eq. (13)—shown in Table 2
DA	The Dubinin–Astakhov equation (Eq. (1))
DC	The determination coefficient
DFT	The density functional theory
DR	The Dubinin–Radushkevich equation (Eq. (1), $n = 2$))
D_{HK}	Constant of Eq. (12)
d	The sum of the diameter of an adsorbent atom and an adsorbate molecule
d_a	The diameter of an adsorbent atom (for carbon is equal to 0.34 nm)
d_A	The diameter of an adsorbate molecule
E_0	The characteristic energy of adsorption calculated from Dubinin–Astakhov equation—Eq. (1)
HK	The Horvath and Kawazoe method
HREM	High-resolution electron microscopy
$J(L-d_a)$	The differential pore size distribution
L	The pore width (diameter)
L	The enthalpy of condensation
L_{av}	The average pore width
$L_{av,I}$	The average effective width of the primary porous structure ($L <\sim 1$) determined from DFT and/or ND
$L_{av,II}$	The average effective width of the secondary porous structure ($\sim 1 < L <\sim 2$) determined from DFT and/or ND
$L_{av,tot}$	The average effective width of the primary and secondary porous structure ($L <\sim 2$) determined from DFT and/or ND
L/d_A	Reduced pore width
$(L-d_a)$	The effective pore width
$(L-d_a)/d_A$	The reduced effective pore width
$(L-d_a)_{p,max}$	The effective pore width related to the maximum value of function $J(L-d_a)$
$(L-d_a)/d_A)_{p,max}$	The reduced effective pore width related to the maximum value of function $J(L-d_a)/d_A)$
MSD	The micropore size distribution
n	The best fit parameter of the Dubinin–Astakhov equation—Eq. (1)
ND	The Nguyen and Do method
p	Equilibrium pressure of an adsorbate
PSD	The pore size distribution
p/p_s	Relative pressure
p_s	Saturation pressure of an adsorbate
p_0	The standard state pressure (= 101325 Pa)
q^{diff}	The differential heat of adsorption
R	Universal gas constant
S	The surface area
SAXS	The small-angle X-ray scattering
S_{BET}	The apparent surface area (calculated in the range of relative pressure ca. 0.05 up to ca. 0.3)
$S_{c,\alpha}$	The total specific surface area calculated from the high-resolution α_s plot (graphitized carbon Sterling FT-G was applied as a reference system)
S_{DA}	The micropore area ($=4 \times 10^3\ W_{0DR}/L_{av}$, where L_{av} is the average micropore width calculated in this case by Eq. (9))
S_{DR}	The micropore area ($=4 \times 10^3\ W_{0DR}/L_{av}$, where L_{av} is the average pore width calculated in this case by Eq. (9))
S_{DFT}	The surface of pores calculated for all the pores ($=S_{DFT}^{micro} + S_{DFT}^{meso}$)
S_{DFT}^{micro}	The surface of pores calculated for all the pores with diameters smaller and/or equal to 2 nm
S_{DFT}^{meso}	The surface of pores calculated for all the pores with diameters larger and/or equal to 2 nm
S^{diff}	The differential molar entropies of adsorbed molecules
S_g	The molar entropy of gas
S_{liq}	The molar entropy of liquid
$S_{me,\alpha}$	The specific surface area of mesopores calculated from the high-resolution α_s plot (graphitized carbon Sterling FT-G was applied as a reference system)
S_{sol}	The molar entropy of solid
T	The temperature
TVFM	Theory of the volume filling of micropores
V	The pore volume
$V_{DFT,I}^{micro}$	The volume of the primary micropores determined from DFT
V_{DFT}^{micro}	The total volume of the micropores with diameters smaller than and/or equal to 2 nm determined from DFT
V_{DFT}^{meso}	The volume of the mesopores with diameters larger than and/or equal to 2 nm determined from DFT
V_{HK}	The micropore volumes determined from HK
$V_{mi,\alpha}$	The volume of micropores calculated from the high-resolution α_s plot (graphitized carbon Sterling FT-G was applied as a reference system)
W	Adsorption
$W_{exp,tot}$	The maximum value of the experimental adsorption (for $p/p_s \approx 1$)

W_0 The volume of micropores calculated from the Dubinin–Astakhov and/or Dubinin–Radushkevich isotherm equation (Eq. (1))

Greek letters

α The coefficient of the adsorbate thermal expansion
β The affinity coefficient
γ Surface tension
ΔH^{ads} The enthalphy of adsorption
ΔS^{ads} The entropy of adsorption
ΔG^{ads} The free energy of adsorption equal to $RT\ln(p/p_s)$
ΔH^{vap} The enthalpy of vaporization
ε Interaction energy
Θ The degree of micropore filling—defined by the Dubinin–Astakhov equation—Eq. (1)
κ The characteristic constant for a defined adsorbate/adsorbent pair in the micropore region
λ The regularization coefficient
ν Liquid molar volume
ρ Liquid density
σ Collision diameter

Subscripts

A Adsorbate
a Adsorbent
all Calculated not only for the range of micropores
mic Calculated only for the range of micropores
ff Fluid–fluid

References

[1] M.M. Dubinin, A.V. Astakhov, Izv. Akad. Nauk SSSR Ser. Khim 5 (1971) 125 (in Russian).
[2] J. Toth, J. Colloid Interface Sci. 163 (1994) 299.
[3] J. Toth, Adv. Colloid Interface Sci. 55 (1995) 54.
[4] G.F. Cerofolini, N. Re, Riv. Del Nuovo Cimento Bologna 16 (1993) 1.
[5] D.D. Do, Adsorption Analysis: Equilibria and Kinetics, ICP, Singapore, 1998.
[6] W. Rudziński, D.H. Everett, Adsorption of Gases on Heterogeneous Surfaces, Academic Press, London, 1992.
[7] P.A. Gauden, A.P. Terzyk, Theory of Adsorption in Micropores of Carbonaceous Materials, WICHiR, Warsaw, 2002 (in Polish).
[8] M. Jaroniec, R. Madey, Physical Adsorption on Heterogeneous Solids, Elsevier, Amsterdam, 1988.
[9] A. Ozawa, S. Kusumi, Y. Ogino, J. Colloid Interface Sci. 56 (1976) 83.
[10] B. Rand, J. Colloid Interface Sci. 56 (1976) 337.
[11] G. Rychlicki, A.P. Terzyk, W. Majchrzycki, J. Chem. Technol. Biot. 74 (1999) 329.
[12] M.M. Dubinin, Carbon 23 (1985) 373.
[13] S.K. Bhatia, H.K. Shethna, Langmuir 10 (1994) 3230.
[14] O. Kadlec, Dokl. Akad. Nauk SSSR 285 (1985) 925.
[15] M.M. Dubinin, H.F. Stoeckli, J. Colloid Interface Sci. 75 (1980) 34.
[16] B. McEnaney, Carbon 25 (1987) 69.
[17] H.F. Stoeckli, L. Ballerini, S. DeBernardini, Carbon 27 (1989) 501.
[18] H.F. Stoeckli, Carbon 27 (1989) 363.
[19] H.F. Stoeckli, F. Kraehenbuehl, L. Ballerini, S. DeBernardini, Carbon 27 (1989) 125.
[20] B. McEnaney, T.J. Mays, in: COPS II Conference, Alicante, 1990.
[21] H.F. Stoeckli, P. Rebstein, L. Ballerini, Carbon 28 (1990) 907.
[22] H.F. Stoeckli, D. Huguenin, A. Laederach, Carbon 32 (1994) 1359.
[23] J. Choma, M. Jaroniec, Karbo-Energochemia-Ekologia 11 (1997) 368 (in Polish).
[24] H.F. Stoeckli, F. Kraehenbuehl, Carbon 22 (1986) 297.
[25] S.G. Chen, R.T. Yang, J. Colloid Interface Sci. 177 (1996) 298.
[26] T. Ohkubo, T. Iiyama, K. Nishikawa, T. Suzuki, K. Kaneko, J. Phys. Chem. 103 (1999) 1859.
[27] P.J.F. Harris, Int. Mater. Rev. 42 (1997) 206.
[28] A.P. Terzyk, P.A. Gauden, G. Rychlicki, R. Wojsz, Carbon 36 (1998) 1703, Erratum, Carbon 37 (1999) 539.
[29] A.P. Terzyk, P.A. Gauden, Colloids Surf. A 177 (2001) 57.
[30] A.P. Terzyk, P.A. Gauden, J. Zawadzki, G. Rychlicki, M. Wiśniewski, P. Kowalczyk, J. Colloid Interface Sci. 243 (2001) 183.
[31] P.A. Gauden, Theoretical Description of the Structural and Energetic Heterogeneity of Carbonaceous Materials, thesis, UMK, Toruń, 2001 (in Polish).
[32] A.P. Terzyk, P. Kowalczyk, P.A. Gauden, G. Rychlicki, S. Ziętek, Colloids Surf. A 201 (2002) 17.
[33] P. Kowalczyk, A.P. Terzyk, P.A. Gauden, L. Solarz, Comput. Chem. 26 (2002) 125.
[34] P. Kowalczyk, A.P. Terzyk, P.A. Gauden, G. Rychlicki, Adsorpt. Sci. Technol. 20 (2002) 295.
[35] A.P. Terzyk, P.A. Gauden, P. Kowalczyk, Carbon 40 (2002) 2879.
[36] J. Jagiełło, J.A. Schwarz, J. Colloid Interface Sci. 154 (1992) 225.
[37] A.P. Terzyk, J. Colloid Interface Sci., in press.
[38] S.G. Chen, R.T. Yang, Langmuir 10 (1994) 4244.
[39] V.K. Dobruskin, Langmuir 14 (1998) 3840.
[40] J.B. Condon, Micropor. Mesopor. Mater. 38 (2000) 359.
[41] J.B. Condon, Micropor. Mesopor. Mater. 38 (2000) 377.
[42] G. Horvath, K. Kawazoe, J. Chem. Eng. Jpn. 16 (1983) 470.
[43] G. Horvath, Colloid Surf. A 141 (1998) 295.
[44] D.H. Everett, J.C. Powl, J. Chem. Soc. Faraday Trans. 72 (1976) 619.
[45] G. Rychlicki, A.P. Terzyk, G. Szymański, Pol. J. Chem. 67 (1993) 2029.
[46] A. Świątkowski, B.J. Trznadel, S. Ziętek, Adsorpt. Sci. Technol. 14 (1996) 58.
[47] T. Ohba, T. Suzuki, K. Kaneko, Carbon 38 (2000) 1879.
[48] T. Ohba, K. Kaneko, Langmuir 17 (2001) 3666.
[49] P. Kowalczyk, L. Solarz, A.P. Terzyk, P.A. Gauden, V.M. Gun'ko, Shedae Informaticae 1259 (11) (2002) 75.
[50] P. Kowalczyk, A.P. Terzyk, P.A. Gauden, R. Leboda, E. Szmechtig-Gauden, G. Rychlicki, Z. Ryu, H. Rong, Carbon 41 (2003) 1113.
[51] P. Kowalczyk, V.M. Gun'ko, A.P. Terzyk, P.A. Gauden, H. Rong, Z. Ryu, D.D. Do, Appl. Surf. Sci. 206 (2003) 67.
[52] P. Kowalczyk, A.P. Terzyk, P.A. Gauden, V.M. Gun'ko, J. Colloid Interface Sci. 256 (2002) 378.
[53] P.A. Gauden, P. Kowalczyk, A.P. Terzyk, Langmuir 19 (2003) 4253.
[54] C.D. Nguyen, D.D. Do, Colloids Surf. A 187 (2001) 51.
[55] V.M. Gun'ko, D.D. Do, Colloids Surf. A 193 (2001) 71.
[56] V.M. Gun'ko, R. Leboda, J. Skubiszewska-Zięba, V.V. Turov, P. Kowalczyk, Langmuir 17 (2001) 3148.
[57] R.J. Dombrowski, D.R. Hyduke, Ch.M. Lastoskie, Langmuir 16 (2000) 5041.
[58] A. Vernov, W.A. Steele, Langmuir 7 (1991) 2817.
[59] D.L. Valladares, F. Rodriguez-Reinoso, G. Zgrablich, Carbon 36 (1998) 1491.
[60] K.T. Thompson, K.E. Gubbins, Langmuir 16 (2000) 5761.
[61] P.B. Balbuena, K.E. Gubbins, Langmuir 9 (1993) 1801.
[62] P.J.M. Carrott, M.M.L. Ribeiro Carrott, T.J. Mays, in: FOA Conference, Paris, 1988.
[63] A. Seri-Levy, D. Avnir, Langmuir 9 (1993) 3067.
[64] Y.F. Yin, B. McEnaney, T.J. Mays, Carbon 36 (1998) 1425.
[65] T. Suzuki, K. Kaneko, N. Setoyama, M. Maddox, K. Gubbins, Carbon 34 (1996) 909.

[66] S.K. Bhatia, Langmuir 18 (2002) 6845.
[67] S. Ismadji, S.K. Bhatia, Langmuir 16 (2000) 9303.
[68] S. Ismadji, S.K. Bhatia, Langmuir 17 (2001) 1489.
[69] R.J. Dombrowski, Ch.M. Lastoskie, D.R. Hyduke, Colloids Surf. A 187–188 (2001) 23.
[70] S.U. Rege, R.T. Yang, AIChE J 46 (2000) 734.
[71] L.S. Cheng, R.T. Yang, Chem. Eng. Sci. 49 (1994) 2599.
[72] A. Saito, H.C. Foley, Micropor. Mater. 3 (1995) 531.
[73] M. Jaroniec, J. Choma, M. Kruk, Colloids Surf. A 214 (2003) 263.
[74] P. Kowalczyk, A.P. Terzyk, P.A. Gauden, Langmuir 18 (2002) 5406.
[75] J. Choma, M. Jaroniec, J.P. Olivier, Przem. Chem. 76 (1997) 101.
[76] J. Choma, M. Jaroniec, Polish J. Chem. 71 (1997) 380.
[77] S. Blacher, B. Sahouli, B. Heinrichs, P. Lodewyckx, R. Pirard, J.P. Pirard, Langmuir 16 (2000) 6754.
[78] J. Zawadzki, M. Wiśniewski, J. Weber, O. Heintz, B. Azambre, Carbon 39 (2001) 187.
[79] J. Jagiełło, J.A. Schwarz, Langmuir 12 (1996) 2837.
[80] K. Wang, D.D. Do, Langmuir 13 (1997) 6226.
[81] B.J. Trznadel, A. Świątkowski, Adsorpt. Sci. Technol. 17 (1999) 303.
[82] R.J. Dombrowski, D.R. Hyduke, Ch.M. Lastoskie, Langmuir 16 (2000) 5041.
[83] C. Nguyen, D.D. Do, Langmuir 16 (2000) 7218.
[84] S. Scaife, P. Kluson, N. Quirke, J. Phys. Chem. B 104 (2000) 313.
[85] P.I. Ravikovitch, A. Vishnyakov, R. Russo, A.V. Neimark, Langmuir 16 (2000) 2311.
[86] K.E. Gubbins, in: J. Fraissard, C.W. Conner (Eds.), Physical Adsorption: Experiment, Theory and Application, Elsevier, Amsterdam, 1997.
[87] G. Rychlicki, Role of Carbon Surface Chemism in Adsorption and Catalytic Processes, UMK, Toruń, 1985 (in Polish).
[88] A.P. Terzyk, The Investigation of Molecular Interactions in the System Adsorbate–Microporous Activated Carbon, thesis, UMK, Toruń, 1995 (in Polish).
[89] A.V. Kiselev, V.P. Dreving, The Experimental Methods in Adsorption and Molecular Chromatography, Izd. Mosk. Univ., Moscow, 1973 (in Russian).
[90] F. Rouquerol, J. Rouquerol, K.S.W. Sing, Adsorption by Powders and Porous Solids: Principles, Methodology and Applications, Academic Press, San Diego, 1999.
[91] G. Rychlicki, A.P. Terzyk, Adsorpt. Sci. Technol. 16 (1998) 641.
[92] G. Rychlicki, A.P. Terzyk, Adsorpt. Sci. Technol. 17 (1999) 323.
[93] K.S.W. Sing, D.H. Everett, R.A.W. Haul, L. Moscou, R.A. Pierotti, J. Rouquerol, T. Siemieniewska, Pure Appl. Chem. 57 (1985) 603.
[94] Lastoskie, N. Qiurke, K.E. Gubbins, in: W. Rudziński, W.A. Steele, G. Zgrablich (Eds.), Equilibria and Dynamics of Gas Adsorption on Heterogeneous Solid Surfaces, Elsevier, Amsterdam, 1997.
[95] P. Kowalczyk, P.A. Gauden, A.P. Terzyk, D.D. Do, G. Rychlicki, Annales UMCS 58 (2002) 46.
[96] W.H. Press, S.A. Teukolsky, W.T. Vetterling, B.P. Flannery, Numerical Recipes in Fortran, Cambridge Univ. Press, Cambridge, UK, 1992.
[97] I. Gajewska, H. Najberg, I. Senderacka, Physicochemical Handbook, Warsaw, WNT, 1961 (in Polish).
[98] K.P. Miszczenko, A.A. Rawdiel, Handbook of the Physicochemical Constants, PWN, Warsaw, 1974 (in Polish).
[99] L. Gardner, M. Kruk, M. Jaroniec, J. Phys. Chem. B 105 (2001) 516.
[100] R. Radhakrishnan, K.E. Gubbins, A. Watanabe, K. Kaneko, J. Chem. Phys. 111 (1999) 9058.
[101] N.N. Avgul, A.V. Kiselev, I.A. Lygina, E.A. Mihailova, Izv. Akad. Nauk SSSR Ser. Khim 5 (1962) 769 (in Russian).
[102] K. Kakei, S. Ozeki, T. Suzuki, K. Kaneko, J. Chem. Soc. Faraday Trans. 86 (1990) 371.
[103] P.A. Webb, C. Orr, Analytical Methods in Fine Particles Technology, Micromeritics Instrument Corp., Norcross, GA, 1997.
[104] M. v. Szombathely, P. Brauer, M. Jaroniec, J. Comput. Chem. 13 (1992) 17.
[105] K. Kaneko, C. Ishii, H. Kanoh, Y. Hanzawa, N. Setoyama, T. Suzuki, Adv. Colloid Interface Sci. 76–77 (1998) 295.
[106] M.M. Dubinin, Adsorption and Porosity, WAT, Warsaw, 1975 (in Polish).
[107] Landolt–Bornstein, Zahlenwerte und Funktionen, Springer-Verlag, Berlin, 1961.
[108] C. Nguyen, D.D. Do, Carbon 39 (2001) 1327.
[109] P.I. Babaev, M.M. Dubinin, A.A. Isirikyan, Izv. Akad. Nauk. SSSR 9 (1976) 1929.
[110] P. Pendleton, J. Colloid Interface Sci. 227 (2000) 227.
[111] A. Watanabe, T. Iiyama, K. Kaneko, Chem. Phys. Lett. 305 (1999) 71.
[112] M.A. Castro, S.M. Clarke, A. Inaba, T. Arnold, R.K. Thomas, J. Phys. Chem. B 102 (1998) 528.
[113] M. Miyahara, K.E. Gubbins, J. Chem. Phys. 106 (1997) 1.
[114] T. Iiyama, K. Nishikawa, T. Suzuki, T. Otowa, M. Hijiriyama, Y. Nojima, K. Kaneko, J. Phys. Chem. B 101 (1997) 3037.
[115] K. Kaneko, A. Watanabe, T. Iiyama, R. Radhakrishan, K.E. Gubbins, J. Phys. Chem. B 103 (1999) 7061.
[116] T. Ohkubo, T. Iiyama, K. Nishikawa, T. Suzuki, K. Kaneko, J. Phys. Chem. B 103 (1999) 1859.